The Center for BRIGHT BEAMS
A National Science Foundation Science & Technology Center

Cryogenic Dark Current in High Gradient RF Guns

Gerard Lawler, Fabio Bosco, Chad Pennington, Jared Maxson, Haoran Xu, Evgenya Simakov, and James Rosenzweig
UCLA, Los Angeles, CA, USA
Cornell University, Ithaca, NY, USA
LANL

UCLA

U.S. DEPARTMENT OF ENERGY

Outline of presentation

1. Background and motivation
2. Electron emission considerations
3. Experimental setup
4. Future testing/discussion
5. Conclusions

1. Background

- High energy linear accelerators like X-ray free electron lasers such as those at SLAC (below) ubiquitous and useful but often large and inaccessible
- PBPL has significant interest in photoinjector, wakefield, and fundamental high field physics
- Broad interest in high gradient cavity development with focus on brightness can reduce scale
- Increase charge with increased quantum efficiency (QE), reduced emittance via reducing energy spread, reducing mean transverse energy (MTE), etc

$$B_{6D} = \frac{2I}{\varepsilon_x \varepsilon_y \varepsilon_z} = \frac{2q}{\varepsilon_x \varepsilon_y \sigma_t \sigma_E}$$

$$\varepsilon_n^2 \propto \langle n^2 \rangle \langle n'^2 \rangle - \langle nn' \rangle^2$$

$$\frac{p_n}{p_z} = \frac{dn}{dz} = n'$$

$$\mathrm{MTE} = \frac{p_\perp^2}{2m}$$

$$QE = \frac{n_e}{n_\gamma} = \frac{h\nu[\mathrm{eV}]}{E_{laser}[\mathrm{J}]} q[\mathrm{C}]$$

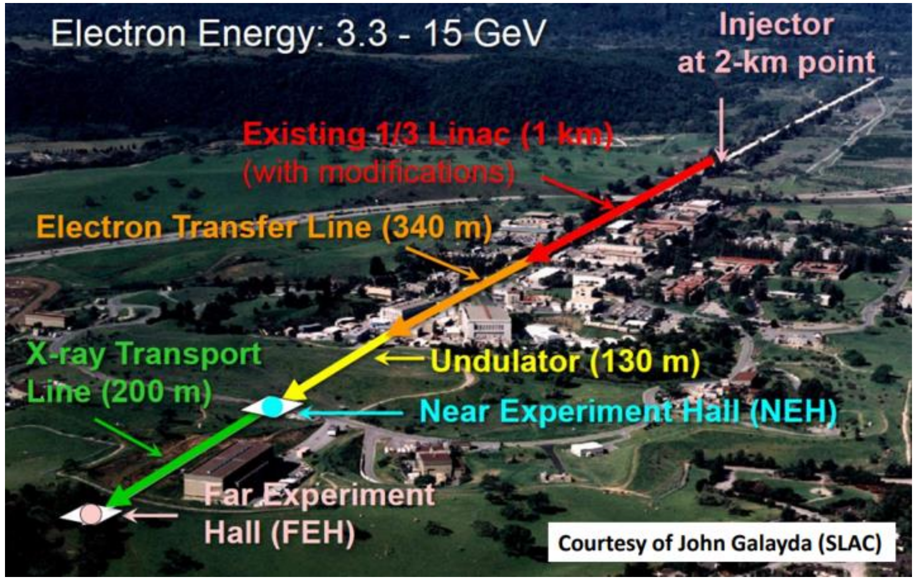

J. Galayda et al., "The new lcls-ii project: Status and challenges," in LINAC, 2014, pp. 404–408. [Online]. Available: https://accelconf.web.cern.ch/linac2014/talks/tuioa04_talk.pdf.

1.6 cell BNL/SLAC/UCLA Cavity E field

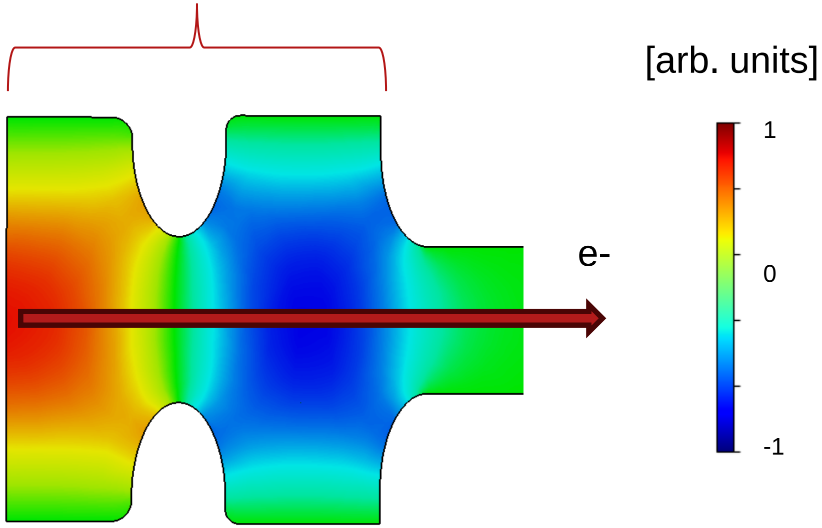

Cryogenic photogun brightness

- Limit to high gradient often breakdown rate (BDR)
- SLAC cryogenic breakdown reduction ⇒ higher accelerating gradients possible
- 1D space charge limited brightness scaling
  - Note launch field and temperature dependence
- *TopGun* previous development in S-band

Rosenzweig, J. B., et al. *Physical Review Accelerators and Beams* 22.2 (2019): 023403.
Doi: 10.1103/PhysRevAccelBeams.22.023403%7

$$B_{e,b} \approx \frac{2ec\varepsilon_0}{k_B T_c}\left(E_0 \sin\varphi_0\right)^2$$

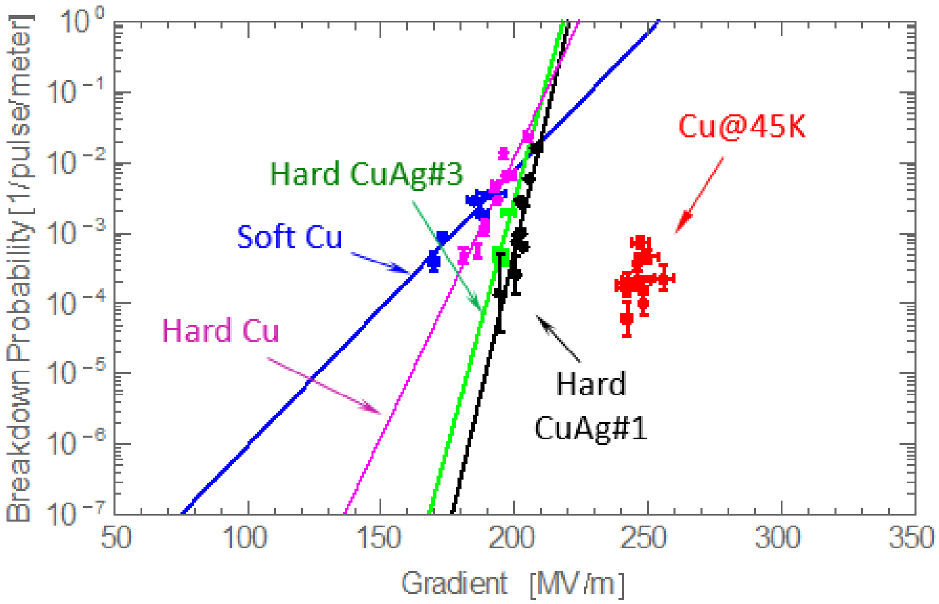

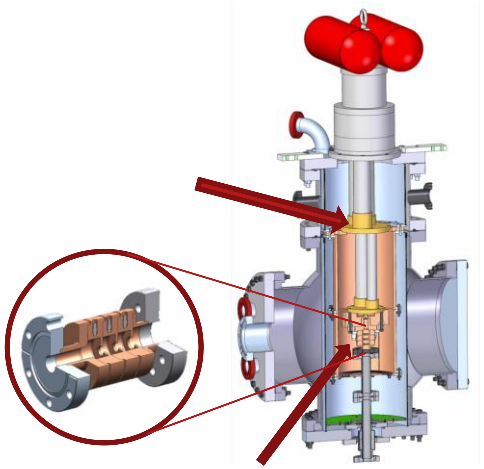

Cavities for high power test

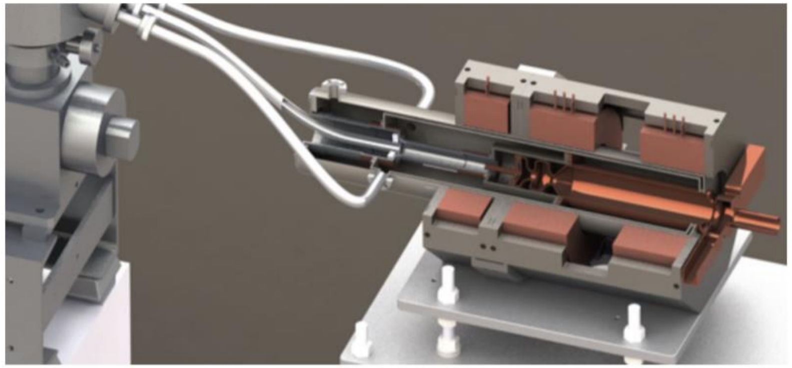

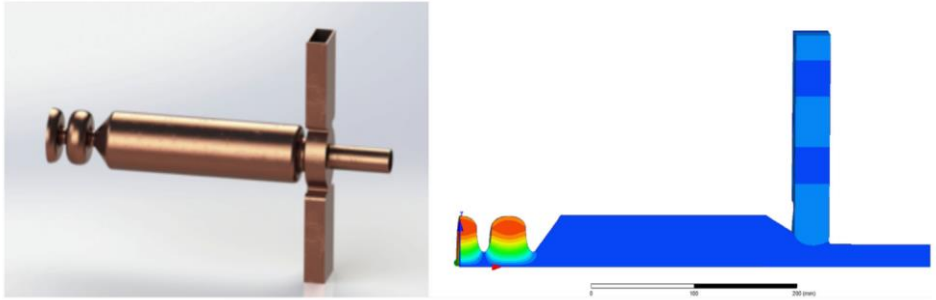

MITHRA Lab and TopGun

- Advertisement for MITHRA 18m of parallel beamline
- Operational with S-band hybrid photoinjector
- Suitable for high energy high gradient linac development (10s-100s MeV); UCXFEL demonstrator FELs; C-band high gradient photoinjector research

J.B. Rosenzweig et al. “A high-flux compact X-ray free-electron laser for next-generation chip metrology needs.” *Preprints* **2023**, 2023111639. https://doi.org/10.20944/preprints202311.1639.v1

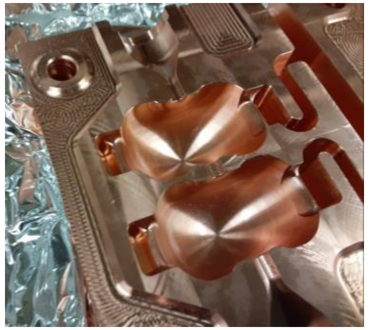

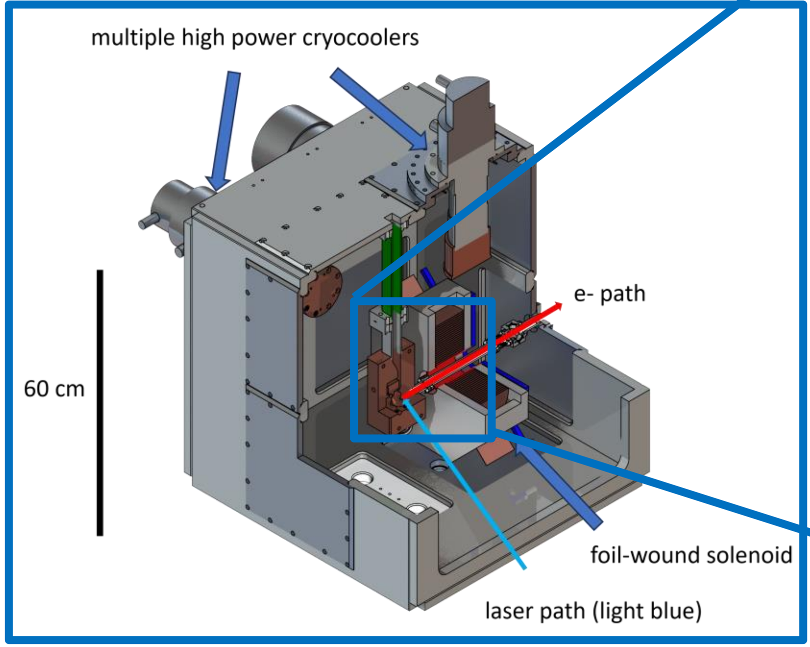

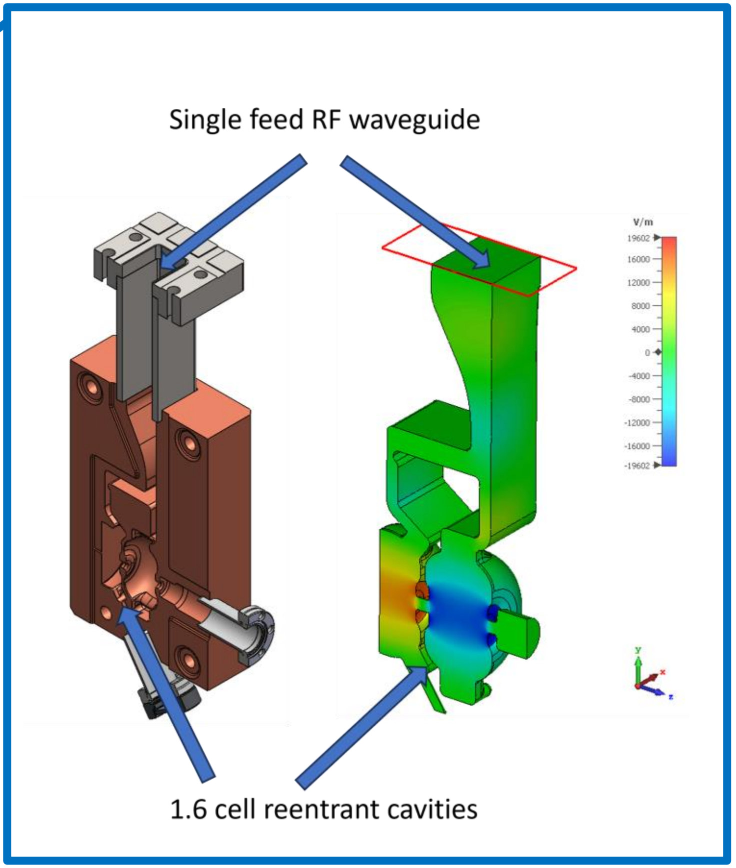

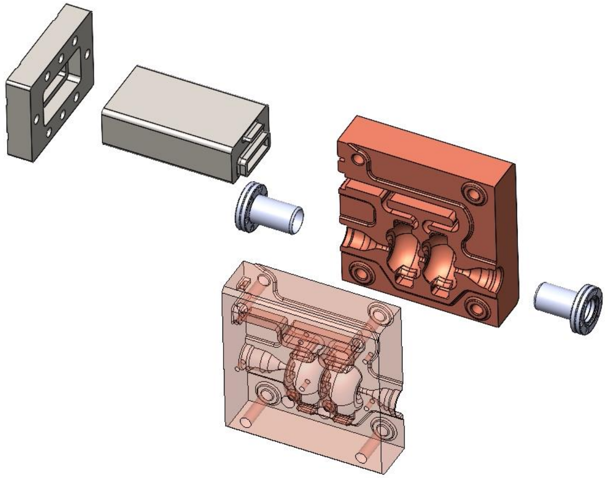

G. Lawler et al., in Proc. NAPAC’22, (Albuquerque, NM, USA), JACoW Publishing, Geneva, Switzerland, Oct. 2022, TUPA81, pp. 516–518, doi: 10.18429/JACoW-NAPAC2022-TUPA81.

UCXFEL

- Our most pertinent realization of high gradient and high brightness techniques is Ultra-Compact Xray FEL (UCXFEL) concept (right)
- When combined with novel bunching and short period undulators we can approach 40m scales with several applications incl. allowing university scale XFEL access and chip metrology
- Existing plan incorporates cryogenically enabled >200 MV/m photoinjector peak fields and ≈ 70 MV/m linacs

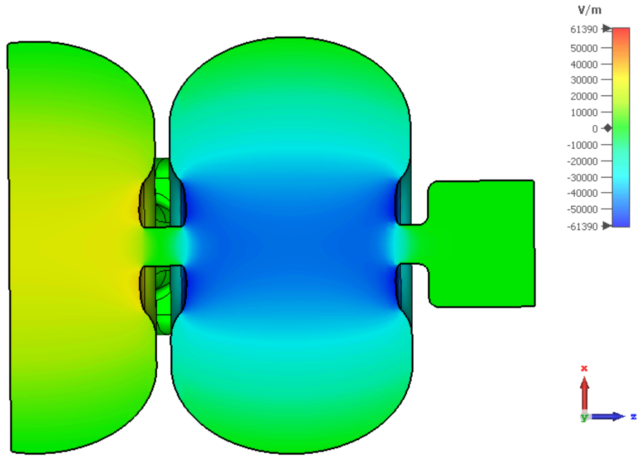

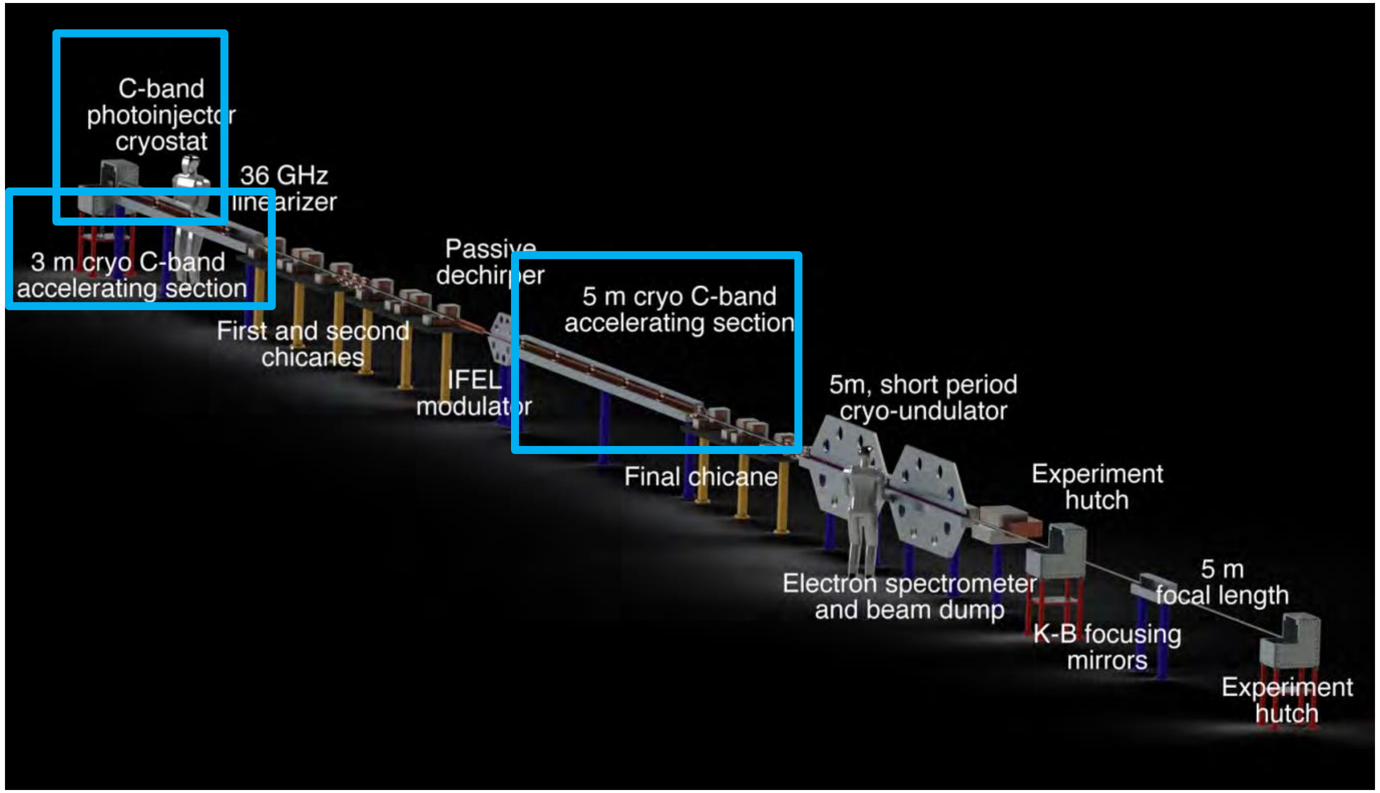

Rosenzweig, J. B. et al., *New Journal of Physics*, vol. 22, no. 9, p. 093067, 2020. `doi:10.1088/1367-2630/abb16c`

Multiobjective optimizations for UED

(a)

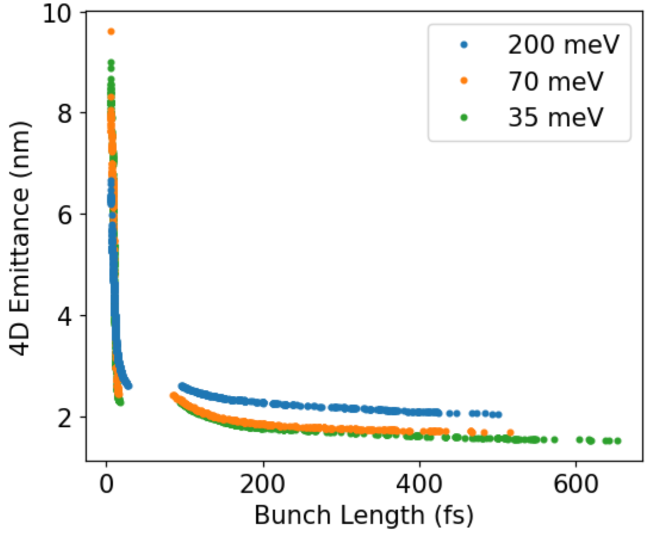

(b)

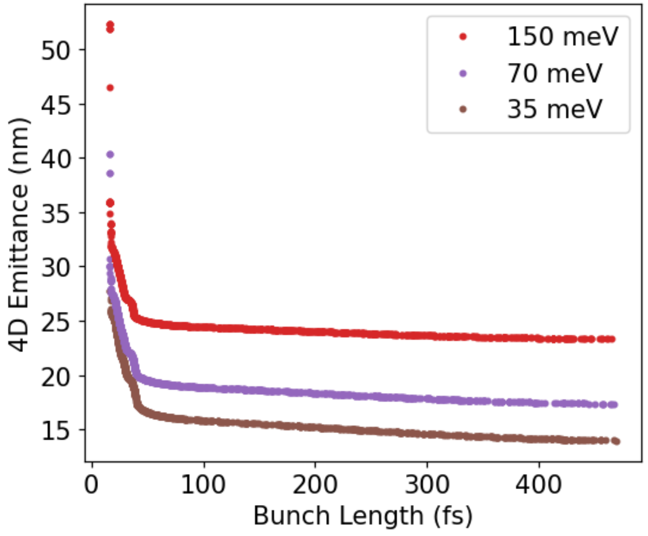

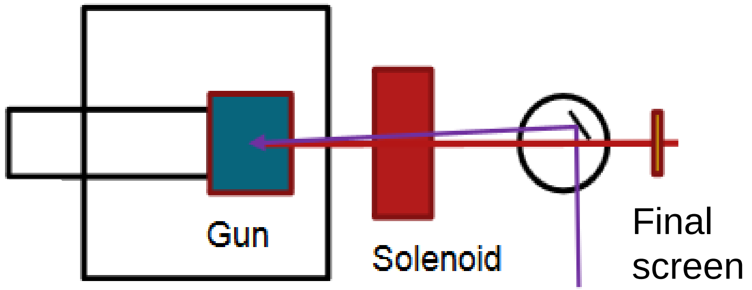

Variables	Range
Gun phase offset ($\Delta\phi$)	[-10, 10] degrees (ϕ_0 = 125 deg)
Solenoid position	[0.24, 0.6] m
Sol strength	[0.0, 3.0] (0.95-> ~0.13 T)
Initial bunch length	[50, 300] fs

Constants	Value
Charge	16 fC
Peak field	180 MV/m
Screen (sample)	1.5 m
Spot size at cathode	(a) 1.2 μm (b) 40.0 μm

Cryo RF Performance Overview

- Parameters for gun thus far compared to RRR100-500 case (left) with empirical numbers measured to inform simulations (right)

Parameter	295K	100K	77K	40K
Frequency	5.695 GHz	5.711 GHz	5.712 GHz	5.713 GHz
Q_0	8579	18668	24200	39812
β	0.7	1.53	1.98	3.26
Filling time	-	0.41 μs	0.45 μs	0.52 μs

Lawler, G. E., et al. *Instruments* 8.1 (2024): 14.
Doi: 10.3390/instruments8010014

E field magnitude

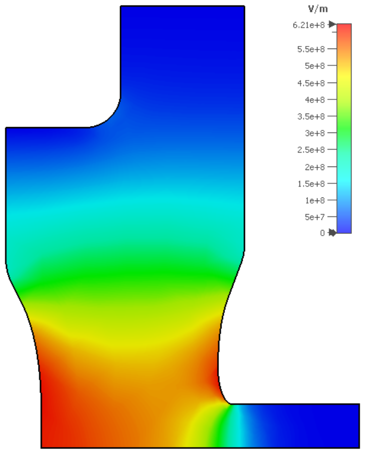

H field magnitude

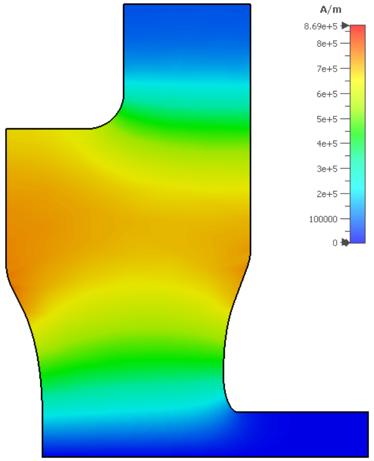

Parameter	295 K	95 K	77K	45 K
f_0 [MHz]	5703.6 ± 0.1[1]	5720.410 ± 0.003[1]	5721 ± 3	5722 ± 4
Q_0	7808 ± 13[1]	14326 ± 12[1]	21000 ± 3600	30000 ± 9900
Coupling β	0.608 ± 0.002[1]	1.069 ± 0.002[1]	1.60 ± 0.44	2.4 ± 0.9
Filling time [μs]	0.271 ± 0.01[1]	0.386 ± 0.001[1]	0.44 ± 0.01	0.49 ± 0.03
Power [MW] for 120 MV/m	1.23 ± 0.10	0.85 ± 0.08	0.79 ± 0.01	0.70 ± 0.09
Energy [J] per 2μs pulse	2.45 ± 0.01	1.70 ± 0.02	1.58 ± 0.03	1.40 ± 0.19
Cathode field @ 0.5 MW	77 ± 3 MV/m	92 ± 5 MV/m	93 ± 3 MV/m	102 ± 7 MV/m

[1] Values experimentally measured or computed directly from low power measurements

Cryo RF Performance Overview

- Parameters for gun thus far compared to RRR100-500 case (left) with empirical numbers measured to inform simulatioı

Parameter	295K	100K	77K	40K
Frequency	5.695 GHz	5.711 GHz	5.712 GHz	5.713 GHz
Q_0	8579	18668	24200	39812
β	0.7	1.53	1.98	3.26
Filling time	-	0.41 μs	0.45 μs	0.52 μs

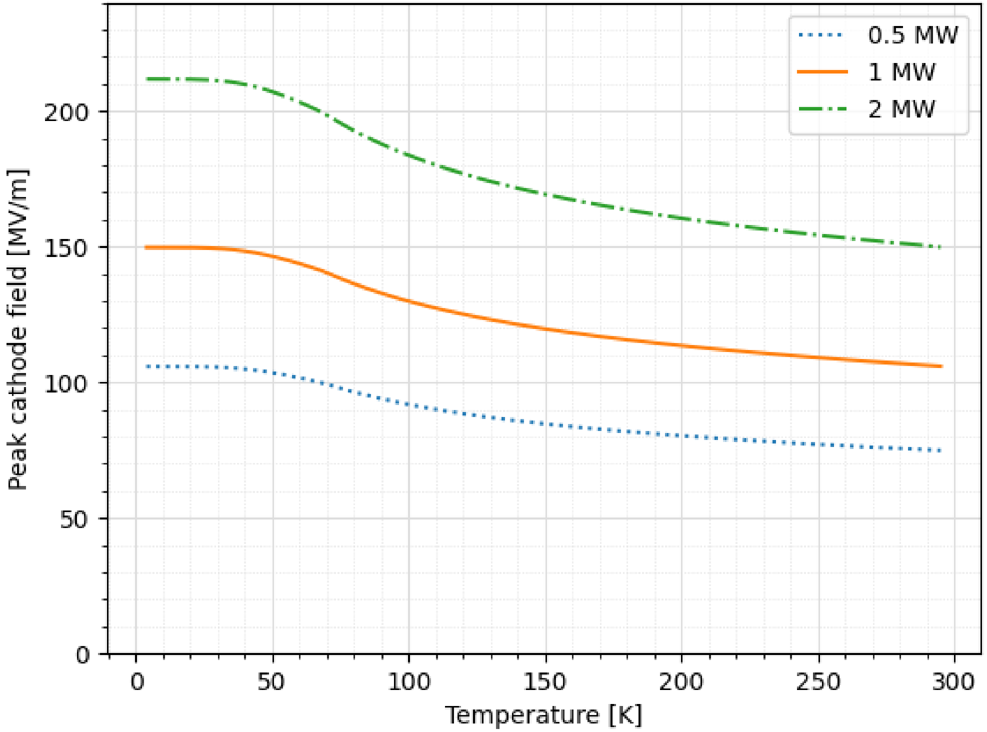

ı (2024): 14.

E field magnitude

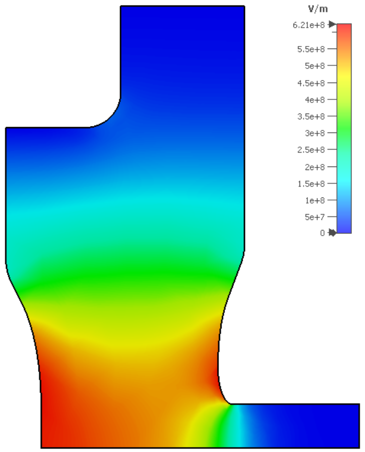

H field magnitude

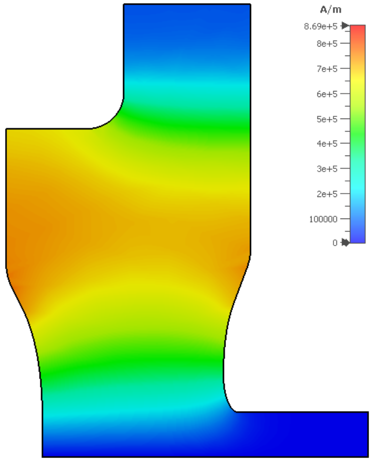

Parameter				45 K
f_0 [MHz]				5722 ± 4
Q_0				30000 ± 9900
Coupling β				2.4 ± 0.9
Filling time [μ				0.49 ± 0.03
Power [MW] for				0.70 ± 0.09
Energy [J] per 2μs pulse				1.40 ± 0.19
Cathode field @ 0.5 MW	77 ± 3 MV/m	92 ± 5 MV/m	93 ± 3 MV/m	102 ± 7 MV/m

[1] Values experimentally measured or computed directly from low power measurements

Gun Comparisons

- CYBORG design inspired primarily by 3 existing photoguns: PEGASUS; Cornell Cryo DC gun; FERMI
- Compared CYBORG design specs also with existing cathode test beds

Parameter	CYBORG Phase 1	CYBORG Phase 2
Cavity type	normal conducting	-
Cavity geometry	$\frac{1}{2}$-cell reentrant	-
Cathode Assembly	Demountable Cu backplate	Cryogenic load lock
Design frequency	5.712 GHz	5.700 – 5.720 GHz
Peak cathode field	$\geq$ 120 MV/m	-
Operating temperature	300 – 95K[1]	300 – 77K

[1] Current lowest temperature achieved with additional plans for 77 K operation

Lawler, G. E., et al. *Instruments* 8.1 (2024): 14.
Doi: 10.3390/instruments8010014

Photoguns	FERMI [20]	PEGASUS [6,21]	PITZ [22,23]	HZDR [24]/HZB [25]	Cornell [26]/ASU [27]	BNL [25,28]
Cavity type *	NCRF	NCRF	NCRF	SRF	-	SRF
Cavity geometry *	1.6 cell pillbox	1.6 cell pillbox	1.5 cell pillbox	1.5 cell elliptical	-	quarter wave
Cathode assembly	Demountable Cu backplate	Demountable Cu backplate + load-lock	Demountable Cu backplate + load-lock	Load-lock	Load-lock	Load-lock
Design frequency	2.998 GHz	2.856 GHz	1.3 GHz	1.3 GHz	DC	0.113 GHz
Peak cathode field	125 MV/m	120 MV/m (Cu backplate)	60 MV/m	15 – 20 MV/m	10 MV/m	10 – 15 MV/m
Min cathode T	$\geq$ room T	$\geq$ room T	$\geq$ room T	80 K	35 K	2 K

* Only relevant for RF guns.

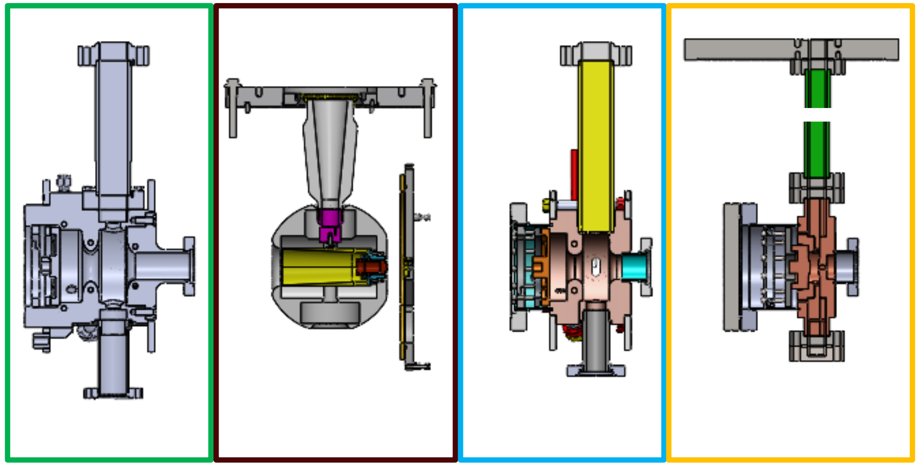

UCXFEL photoinjector Gun Comparisons

- CYBORG design insp d primarily by 3 exis PEGASU FERMI
- Compare also with

Parameter	CYBORG Phase 1	CYBORG Phase 2
	normal conducting	-
	$\frac{1}{2}$-cell reentrant	-
	Demountable Cu backplate	Cryogenic load lock
	5.712 GHz	5.700 – 5.720 GHz
	$\geq$ 120 MV/m	-
	300 – 95K[1]	300 – 77K

[1] with additional plans for 77 K operation

Lawler, G. E., et al. *Instruments* 8.1 (2024): 14.
Doi: 10.3390/instruments8010014

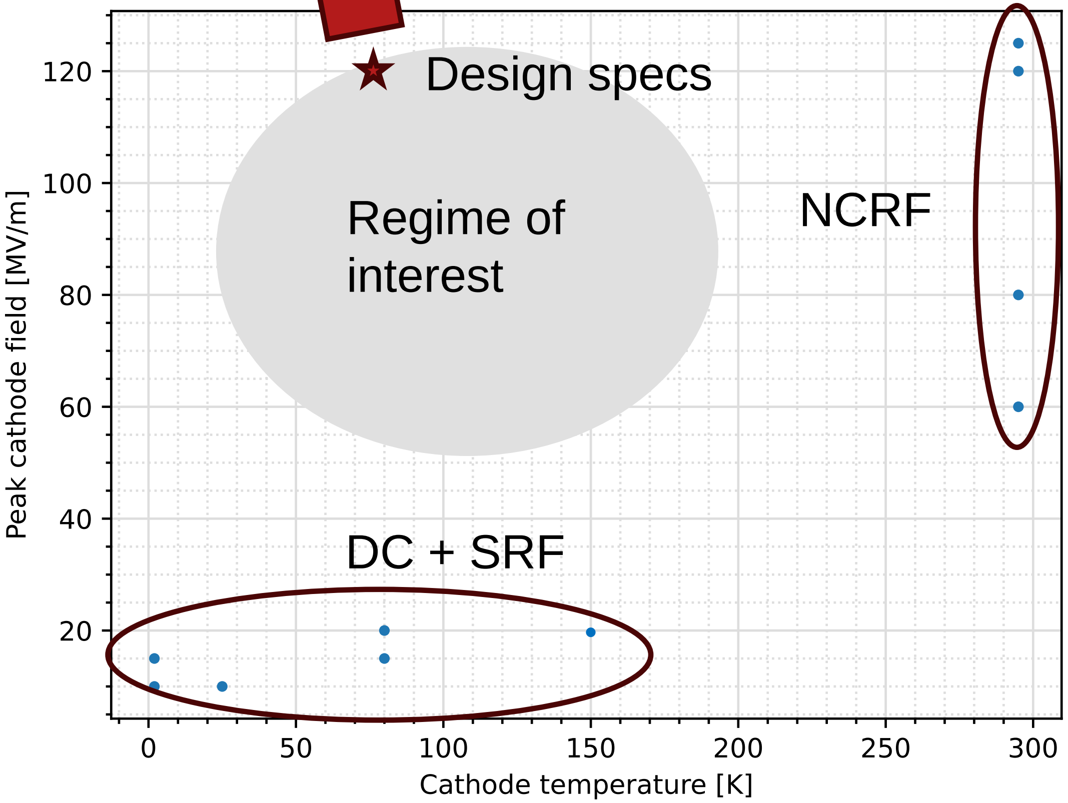

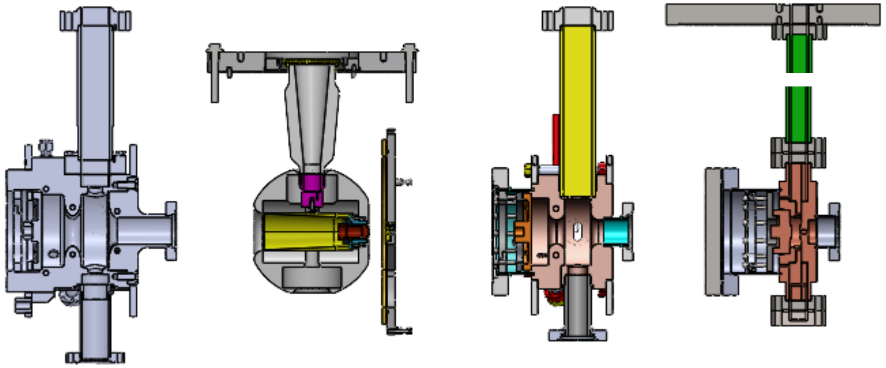

Photoguns	FE					
Cavity type *						
Cavity geometry *	1.6					
Cathode assembly	Der Cu					
Design frequency	2.					
Peak cathode field	12					
Min cathode T	$\geq$ room T	$\geq$ room T	$\geq$ room T	80 K	35 K	2 K

* Only relevant for RF guns.

2. Dark current simulation

- Fowler-Nordheim field emission in particle-in-cell (PIC) simulation via CST with peak cathode plane nosecone gradient 60 MV/m and β = 50 needed for significant emission

$$\bar{I}_F = \frac{1}{T}\int_0^T I_F(t)dt$$

$$= \frac{1.54\times 10^{-6} A_e \beta^2 E_0^2 10^{4.52\phi^{-0.5}}}{\phi}\frac{2}{T}$$

$$\int_0^{\frac{T}{4}} \sin^2 \omega t \exp\left(-\frac{6.53\times 10^9 \phi^{1.5}}{\beta E_0 \sin \omega t}\right) dt$$

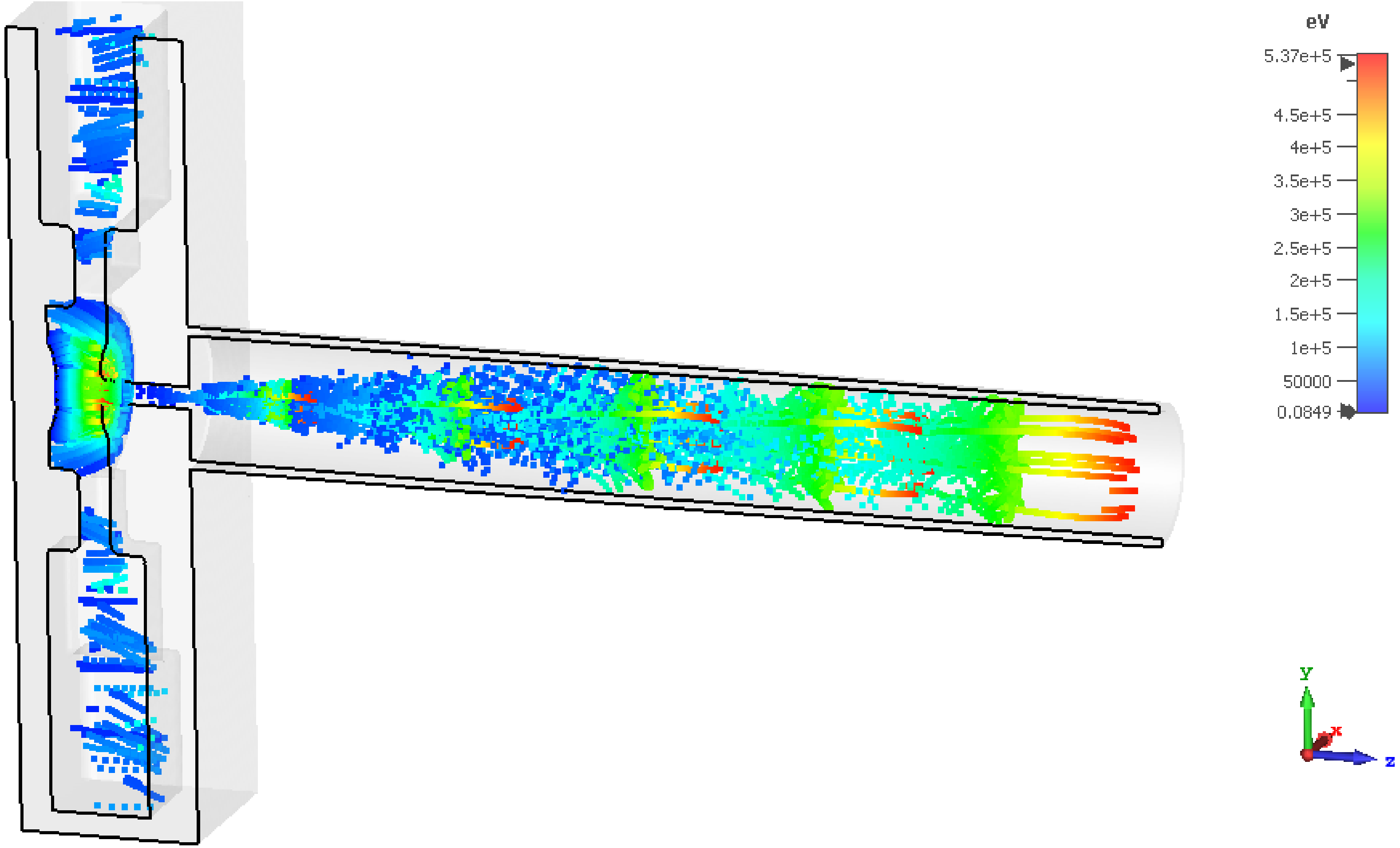

Dark current simulation

- Considering peak electric field enhancement optimized on nosecone, down stream dark current emission mostly localized to nosecone
- Isolated nosecone emission (right) showing additional collimation from iris and beam pipe

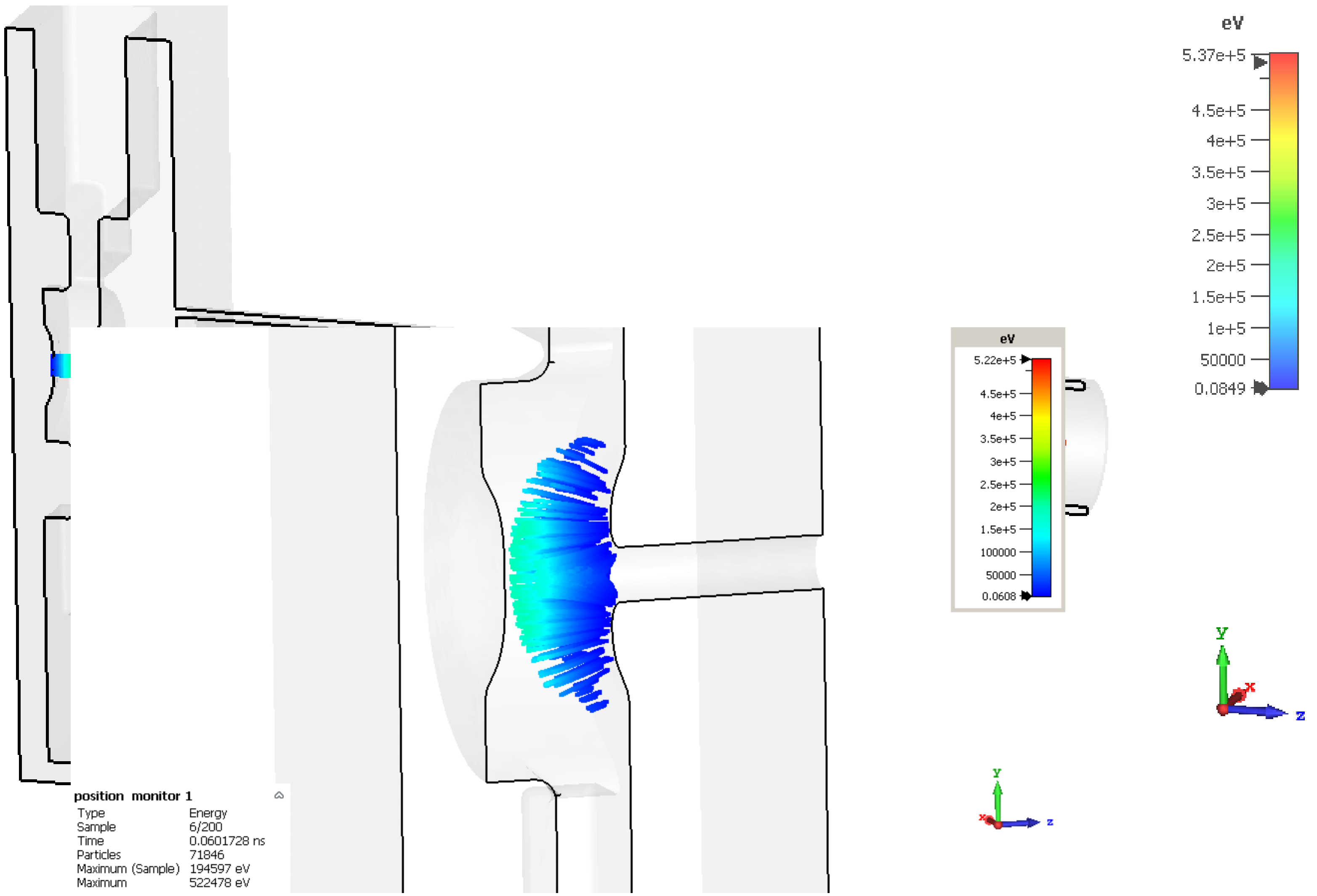

TF emission

- Rather than Fowler –Nordheim for completeness use a general thermal-field emission model via Jensen that incorporates thermionic and field emission contributions

$$J_{GTF}(F,T) = \begin{cases} n^{-2}J_F + J_T & (n < 1) \\ J_F + n^2 J_T & (n > 1) \end{cases}$$

Jensen, Kevin L., and Marc Cahay. "General thermal-field emission equation." *Applied physics letters* 88.15 (2006).

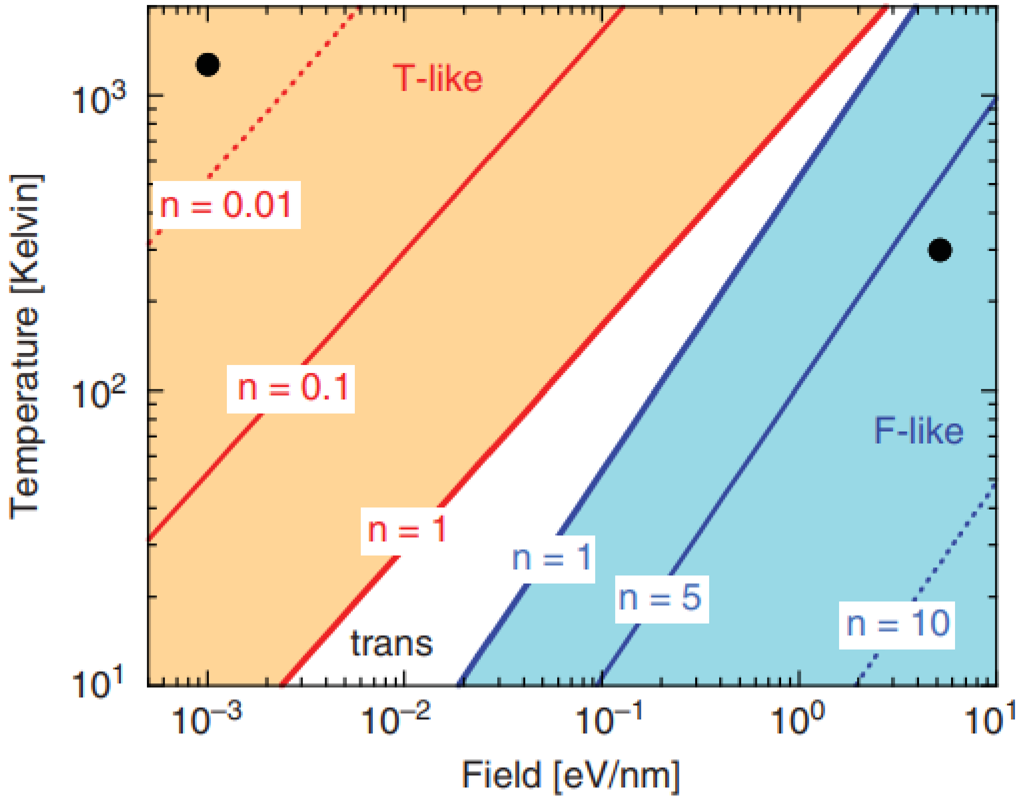

TF emission

- Rather than Fowler –Nordheim for completeness use a general thermal-field emission model via Jensen that incorporates thermionic and field emission contributions

$$J_{GTF}(F,T) = \begin{cases} n^{-2} J_F + J_T & (n < 1) \\ J_F + n^2 J_T & (n > 1) \end{cases}$$

Jensen, Kevin L., and Marc Cahay. "General thermal-field emission equation." *Applied physics letters* 88.15 (2006).

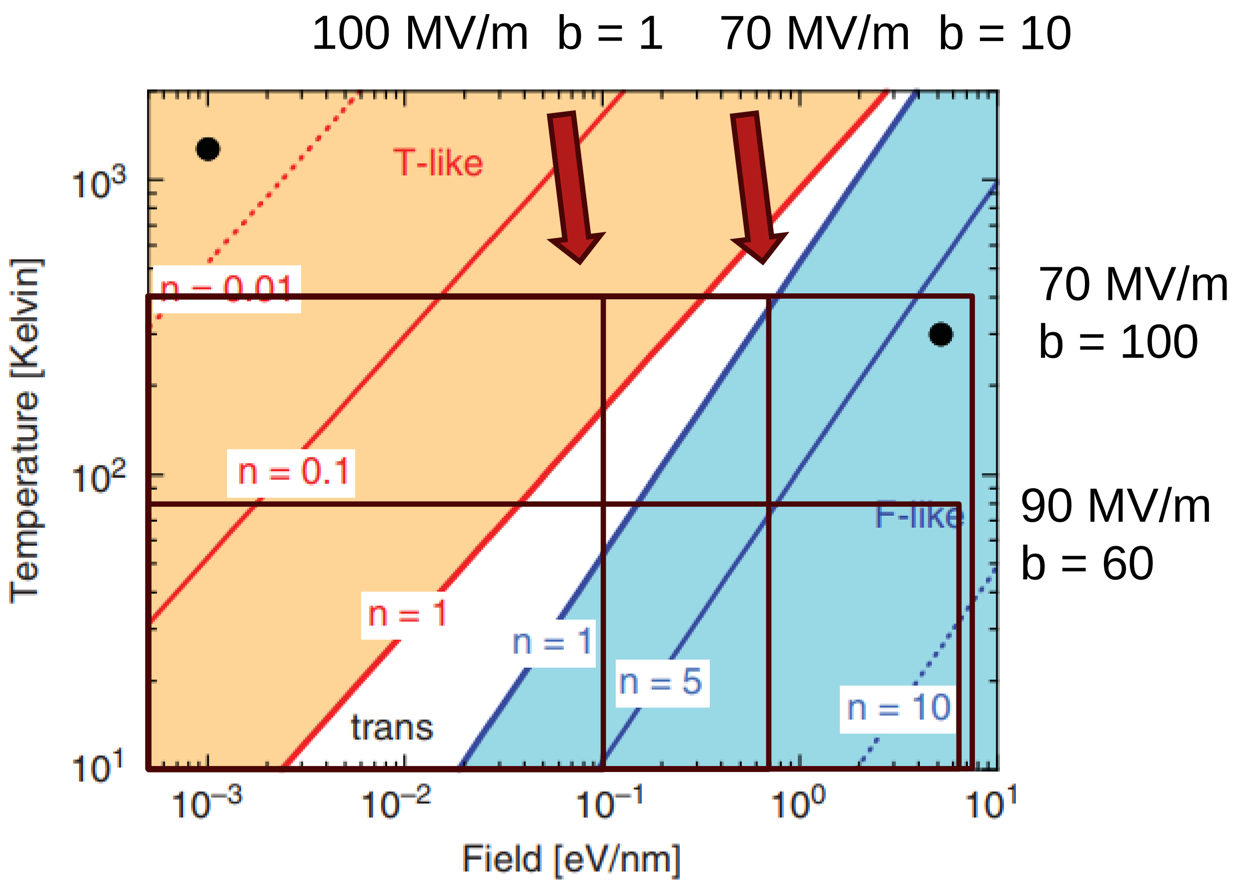

TF emission

- Pulse heating needed to achieve some reasonable visible effect (400 K)
- But Cu melts at certain temperatures

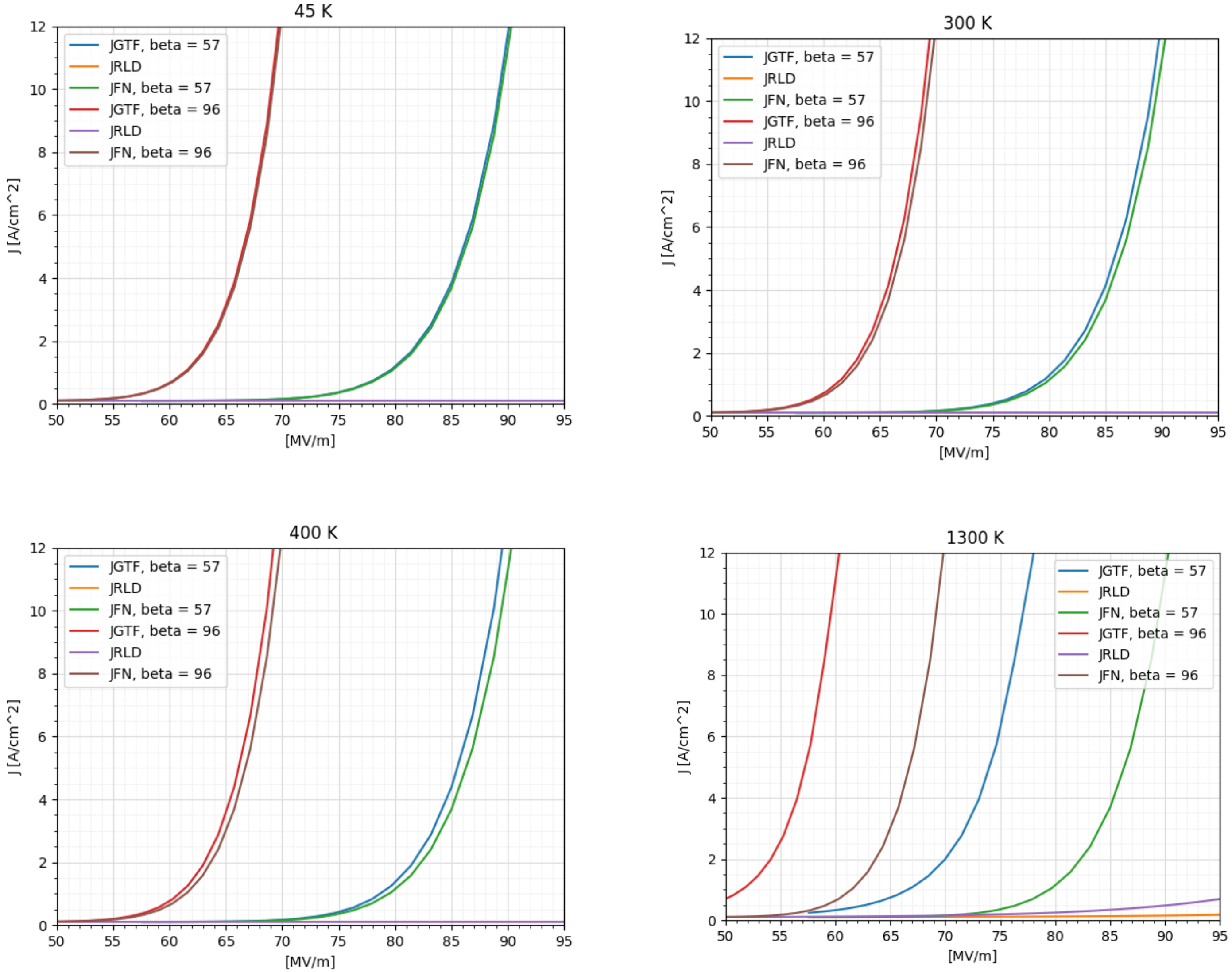

CYBORG Phase1

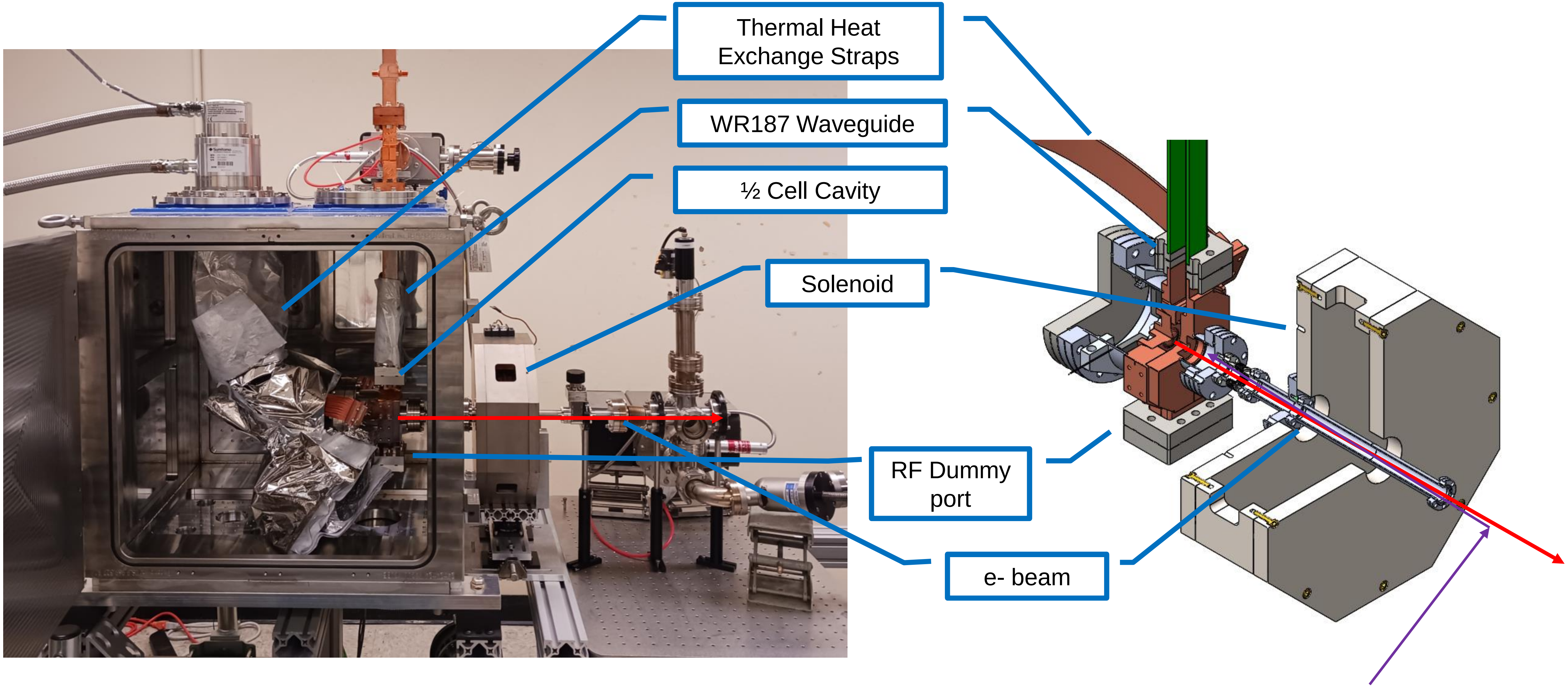

CYBORG Phase1 (cont.)

- Added preliminary beamline section sufficient for gun conditioning: **(a,e)** 2x ion pumps , **(b)** solenoid, **(c)** steering magnet **(d)** YAG screen
- < 10^-8 torr (2uA; 5 uA) at gun and screen
- Custom solenoid mount has 4 degrees of freedom
  - 3 transverse + rotation about x (vertical axis)

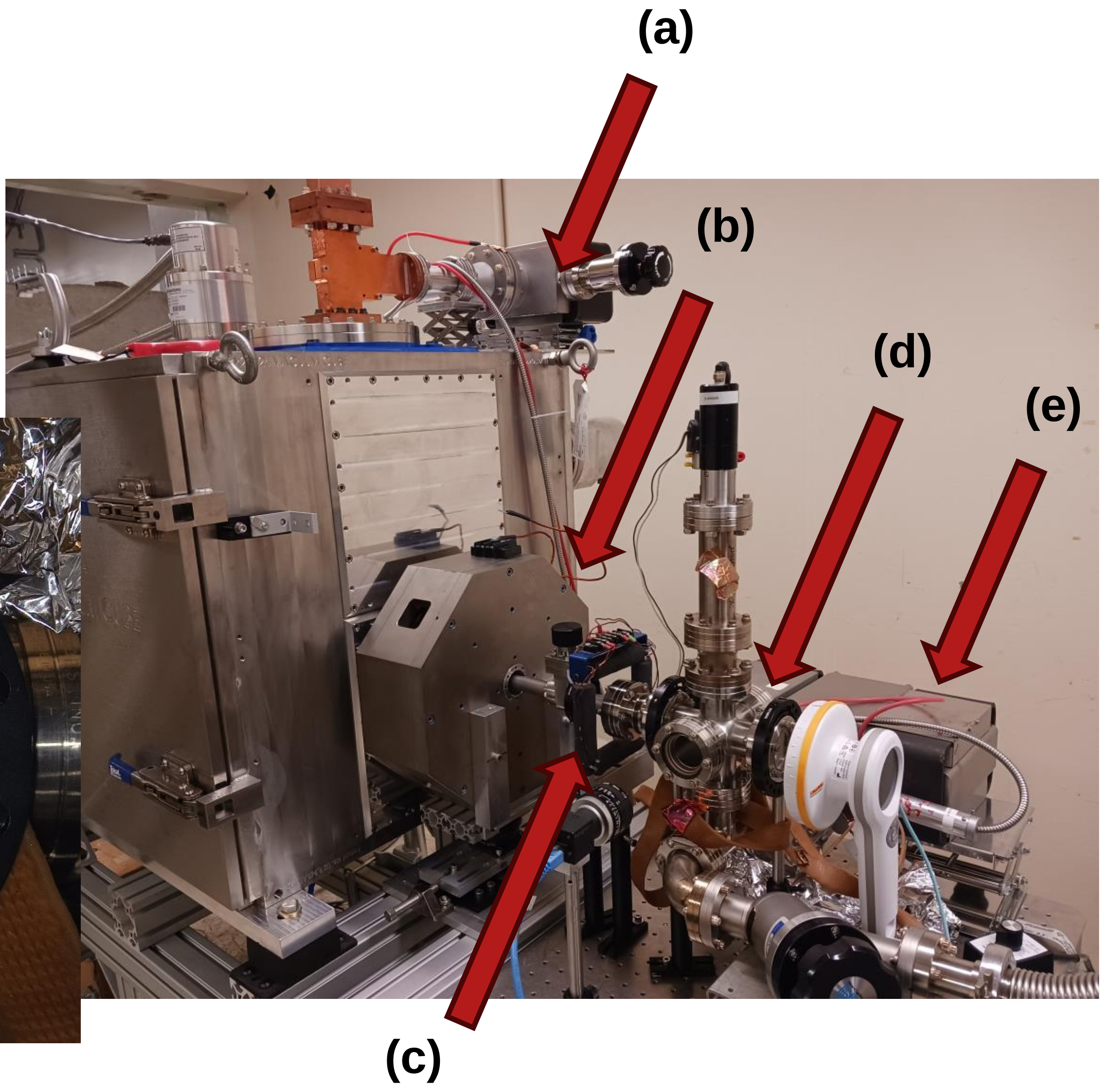

Cu cathode visible down the barrel of the gun

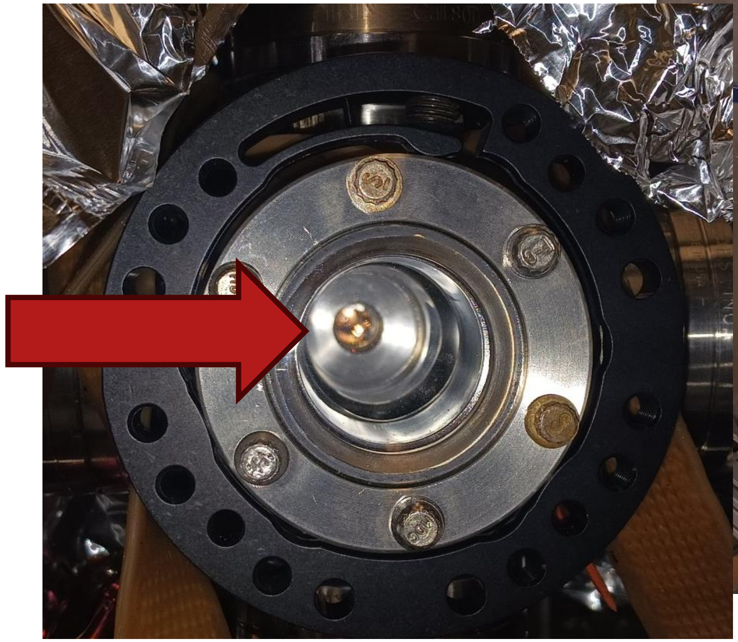

Gun topology

- Comparison of possible topologies originally considered shown below

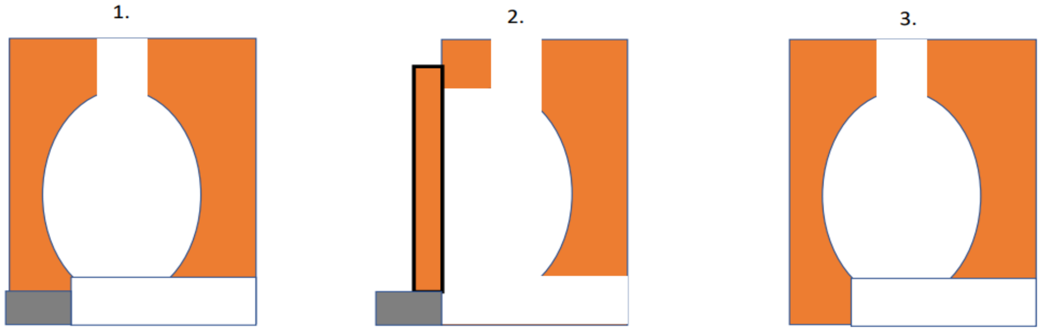

- Plug directly into cavity
- Useful for 1.6 cell to max gradient

- Good for cathode tests
- High gradient (120 MV/m) but lower than plug alone

- No cathode exchange
- Highest achievable gradients

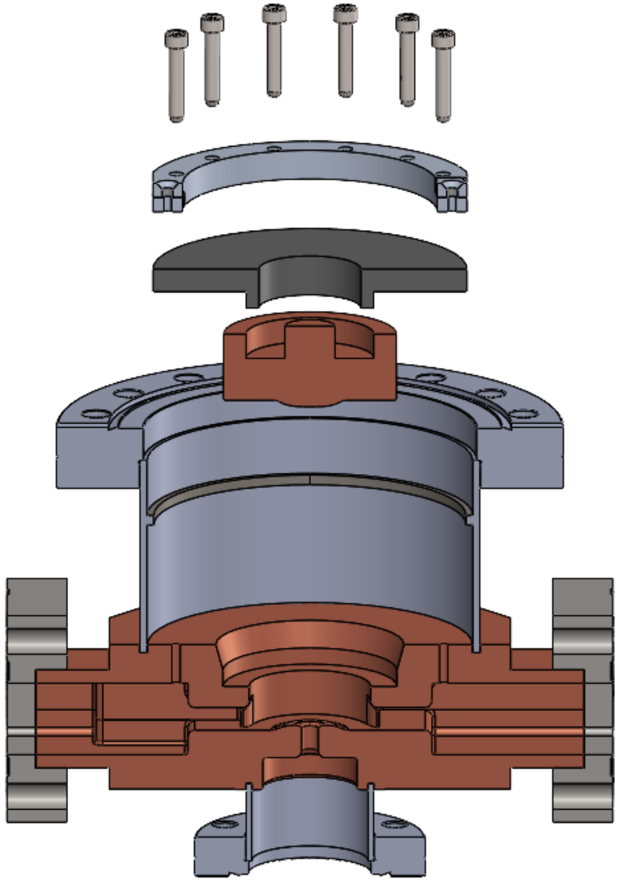

- Design philosophy of gun focused on maximum versatility
- Original design for fully removable backplane focused on allowing testing of multiple cathode insertion coupling designs
- Further useful for examination of cavity surface after field emission and breakdown

Cryogenic Dark Current

- Approximate total charge can be estimated via *beam loading* i.e. measured loss in Q0 from expected values in presence of excess charge giving approx. 10s pC
- From additional PIC simulation analysis, 7-8% of electrons make it >30 cm downstream, so < 1 pC expected downstream (25+ cm)
- 10-100 pC/2 us = 5-50 uA total and 0.5 pC expected downstream
- 500 uA in LCLS, 50 uA in SwissFEL, 10 uA in superconducting EuXFEL (2 m downstream)

G. Shu et al, *Nuclear Instruments and Methods in Physics Research Section A: Accelerators, Spectrometers, Detectors and Associated Equipment*, Volume 1010, 2021,165546, ISSN 0168-9002, doi:10.1016/j.nima.2021.165546.

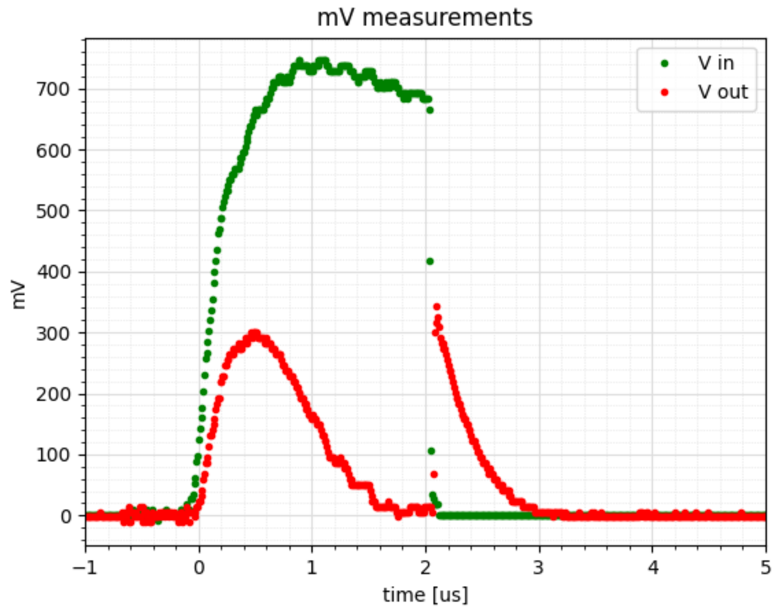

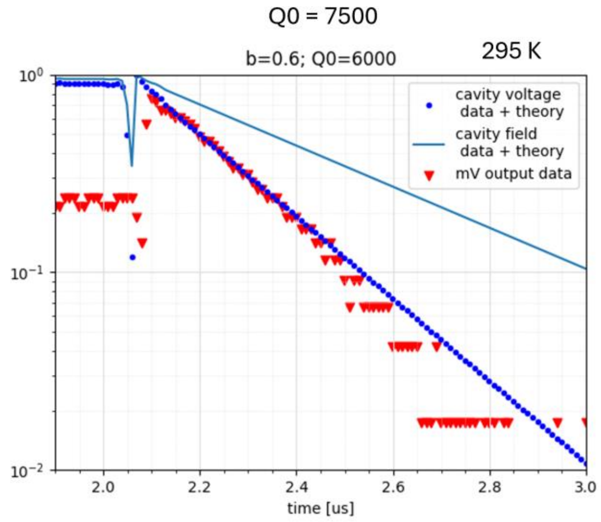

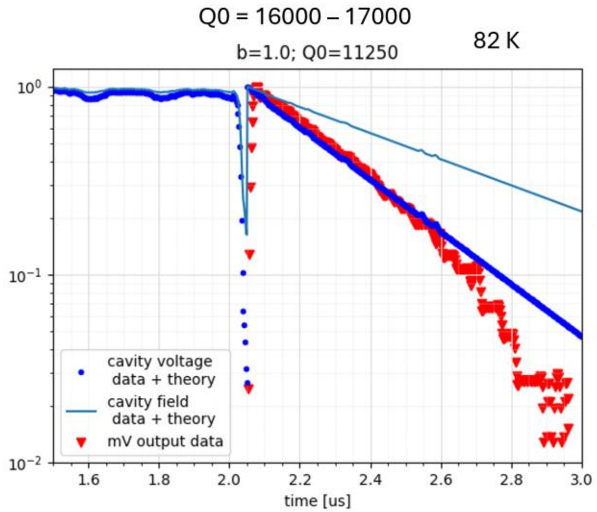

Peak RF Performance

- Maximum RF input power currently into gun between 450 – 520 kW with fluctuation, stable at 450 kW
- Max peak field estimate >90 MV/m at 85K and 78 MV/m at room temperature
  - Determined with two different methods reflected pulse QL calculation and using coupling + Q0 from low power test
- Plots below show dark current scaling which show significant improvement of field possible using same input RF power
- YAG screen dark current measurements at approximately same input power

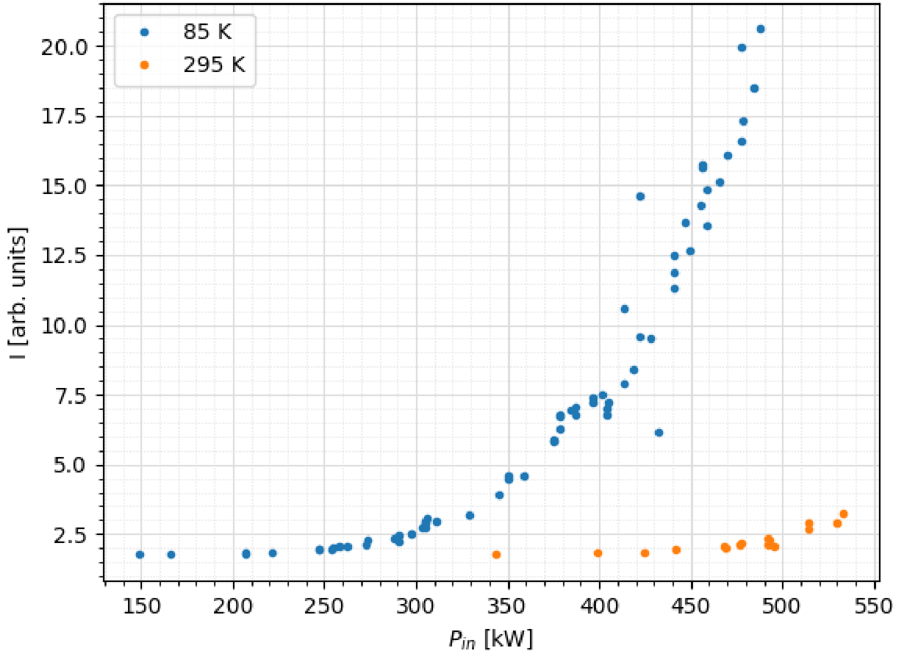

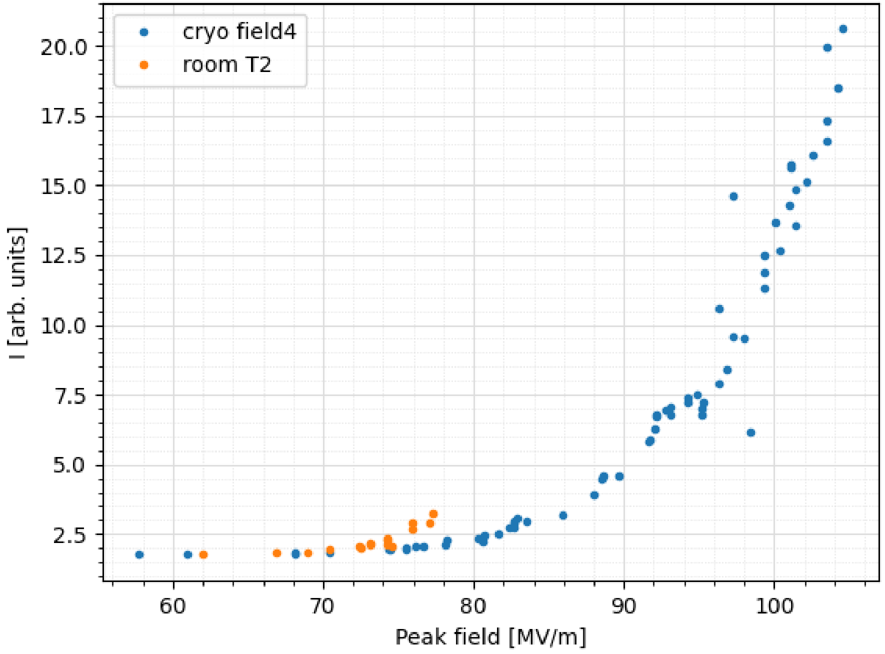

70 MV/m @ 295 K

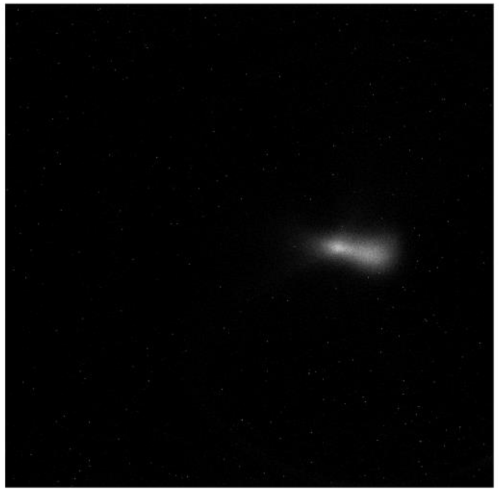

95 MV/m @ 82.5 K

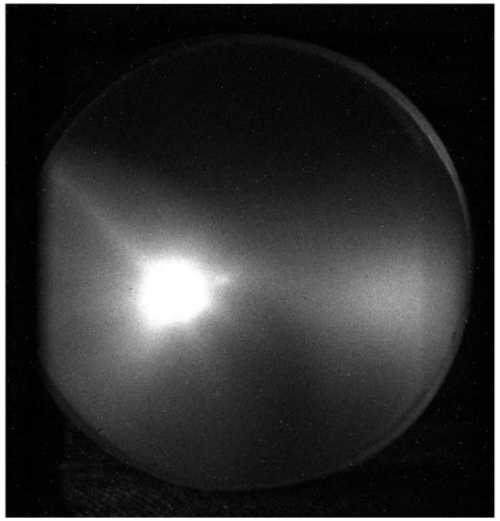

Dark current temperature dependence

- Cryogenic pulsed DC experiments show temperature dependence (below)
- Begun to see similar results in CYBORG during high field conditioning (right)

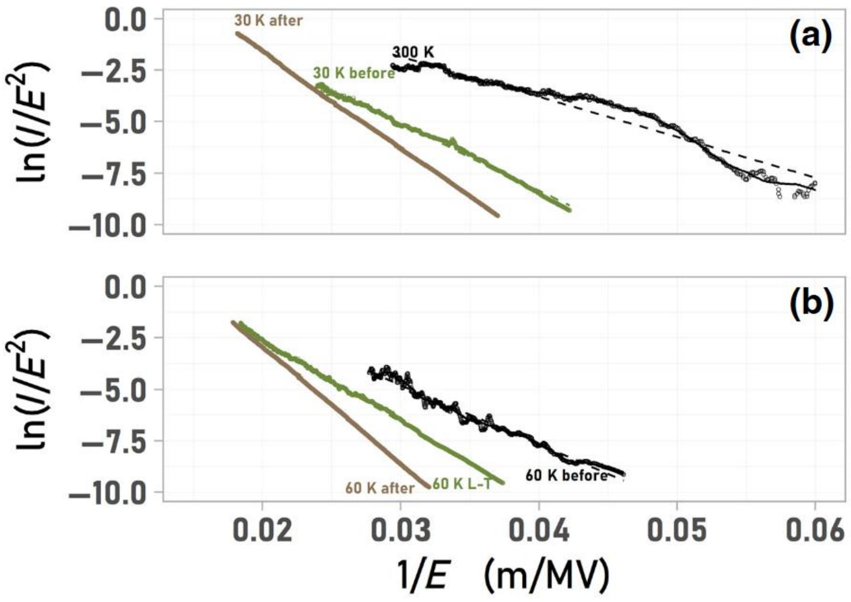

Jacewicz, Marek, et al. "Temperature-dependent field emission and breakdown measurements using a pulsed high-voltage cryosystem." *Physical Review Applied* 14.6 (2020): 061002.

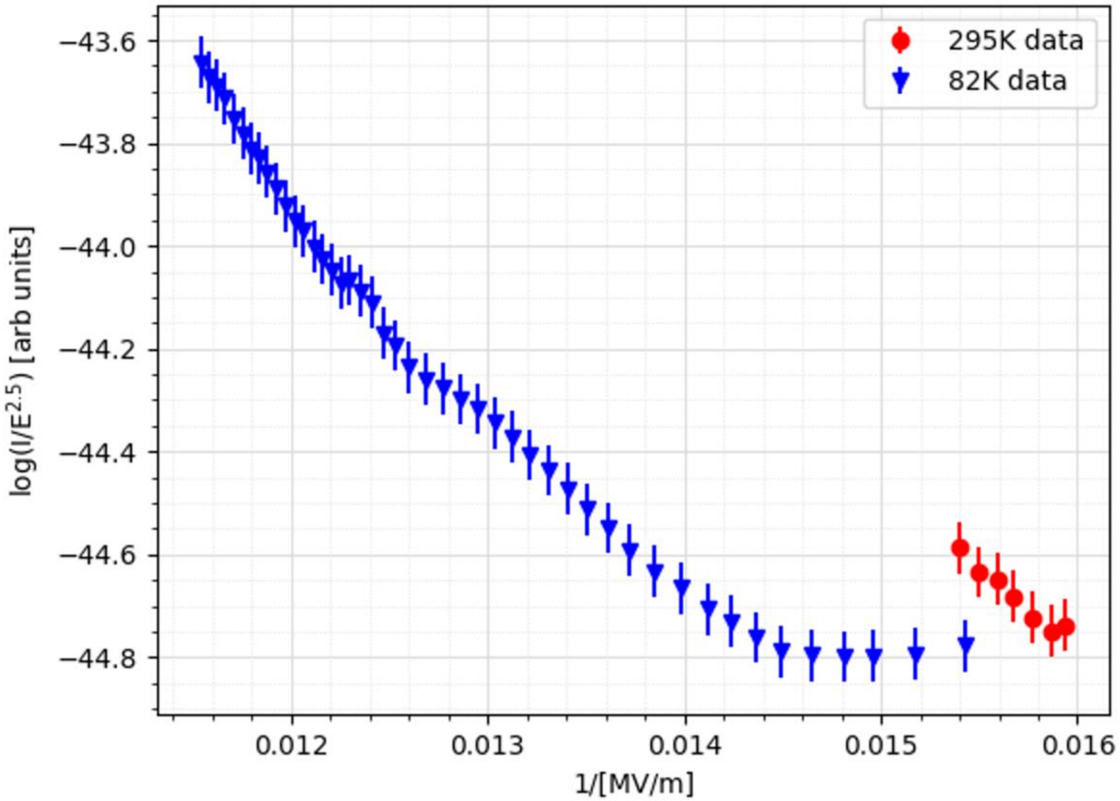

Dark current temperature dependence

- Effective enhancement appears reduced for higher fields
- Data has implicit time dependence on scale of hours at 1 Hz rep rate so may represent also an effect of conditioning
- More data needed

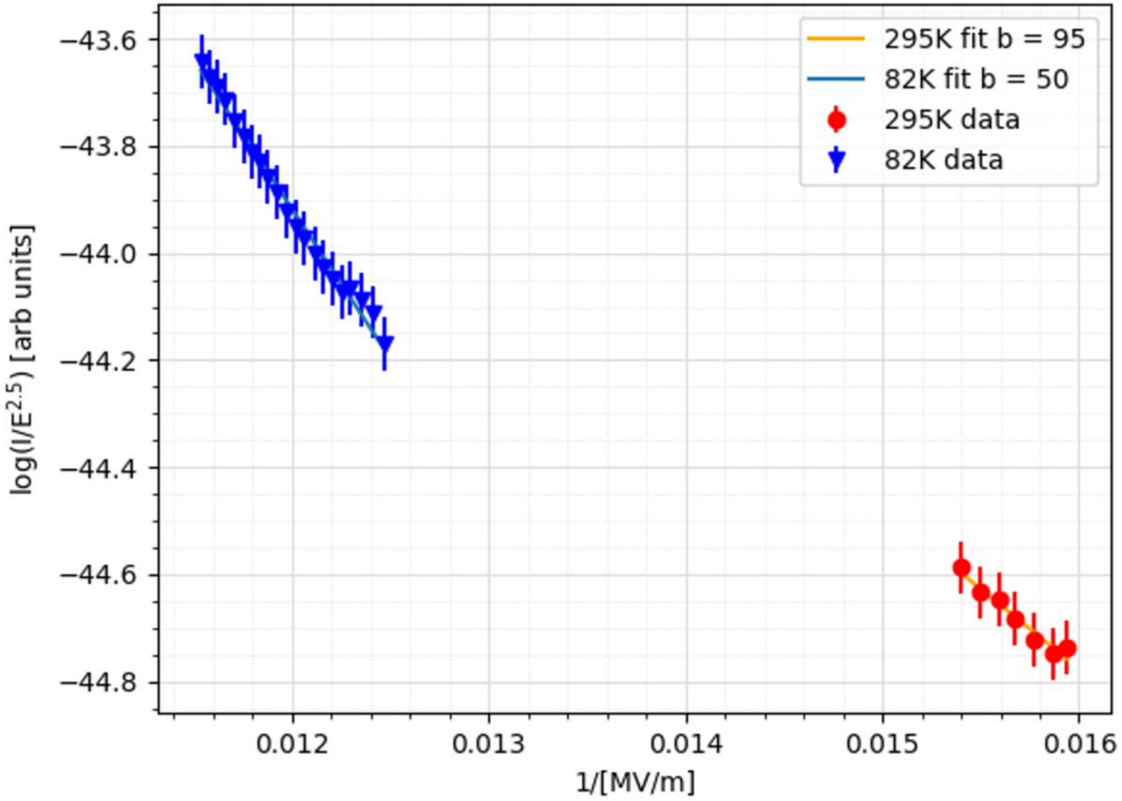

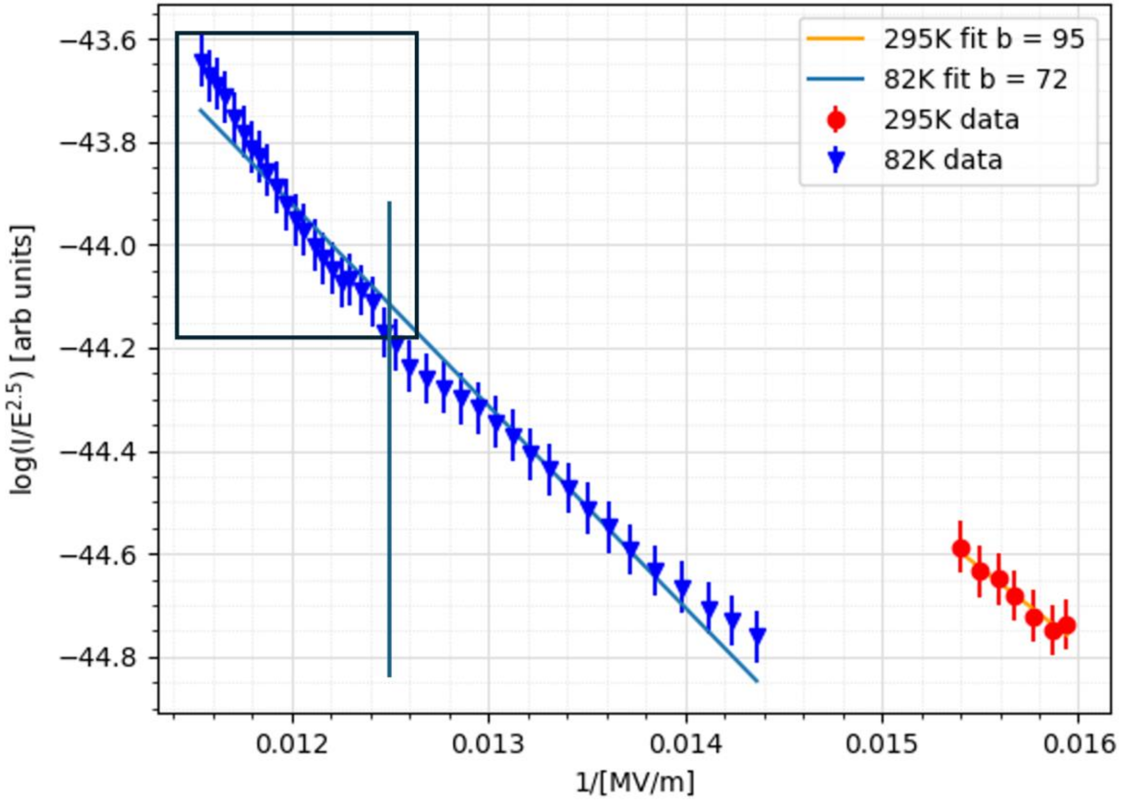

Dark current temperature dependence

- Effective enhancement appears reduced for higher fields
- Data has implicit time dependence on scale of hours at 1 Hz rep rate so may represent also an effect of conditioning
- More data needed

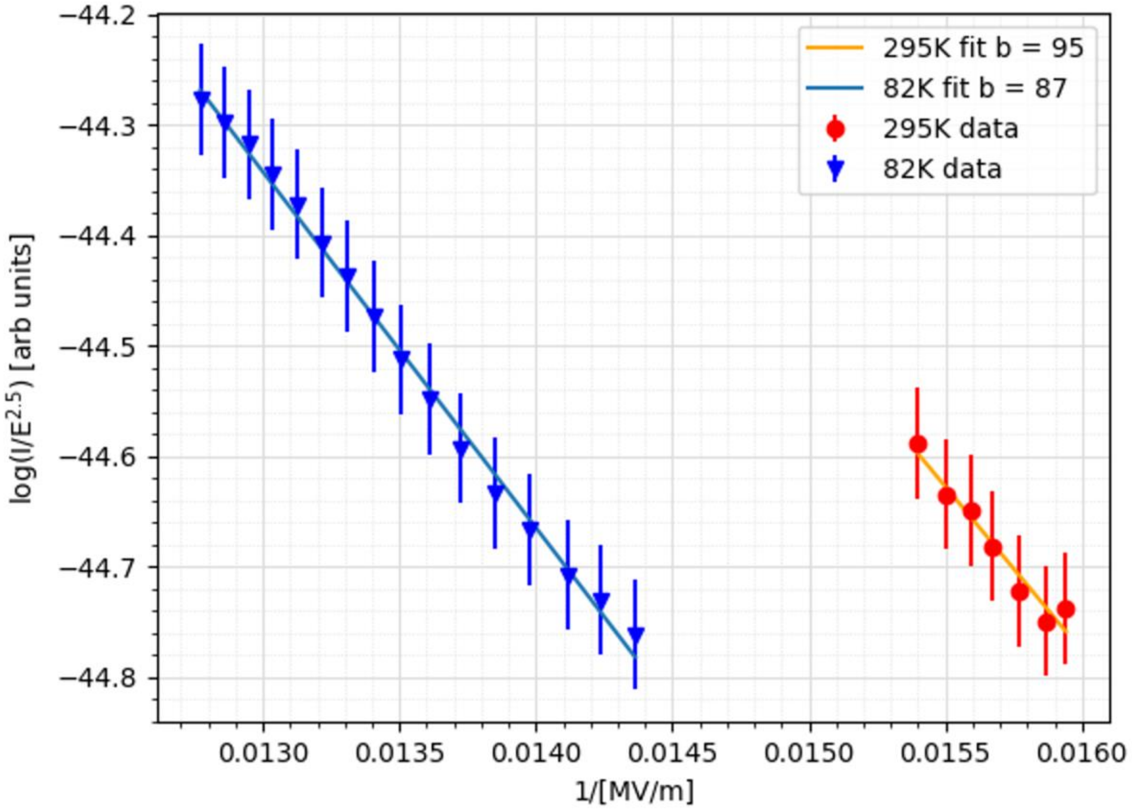

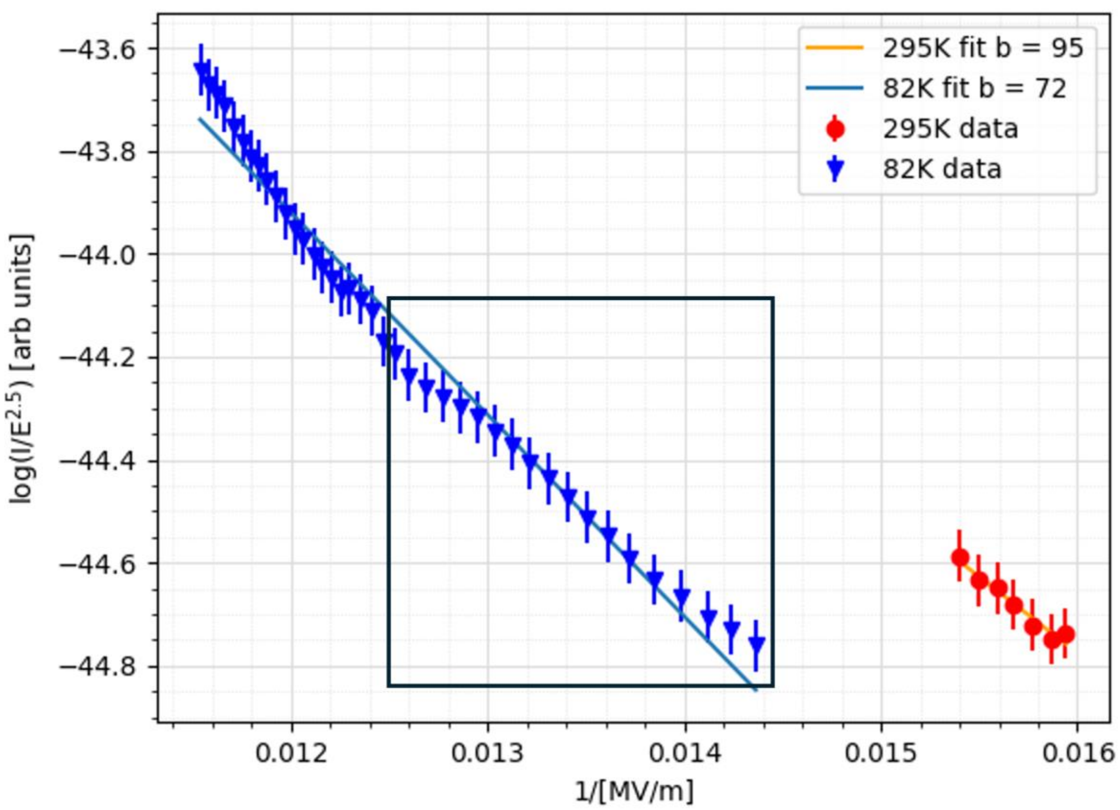

Emission tip toy model

- Temperature dependence not present in Fowler-Nordheim tunneling
- Useful simple model, taking effective β, and scaling field to get geometric deformation empirically to obtain room temperature value
- Then using NIST Young’s modulus and Poisson ratio for copper to obtain reduced field enhancement geometry at low temperatures due to increased material hardness

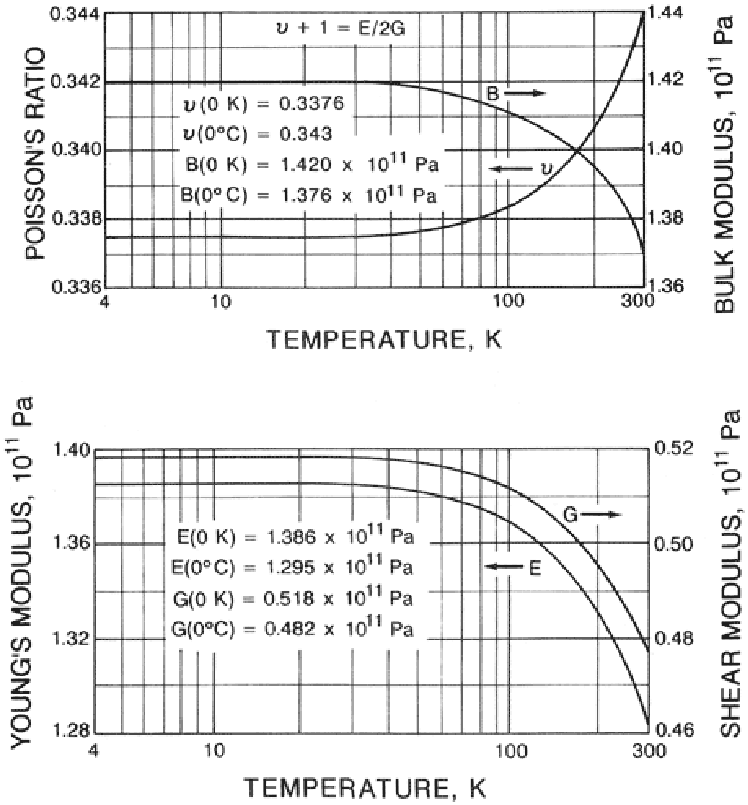

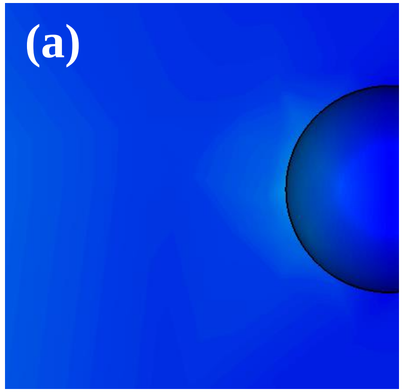

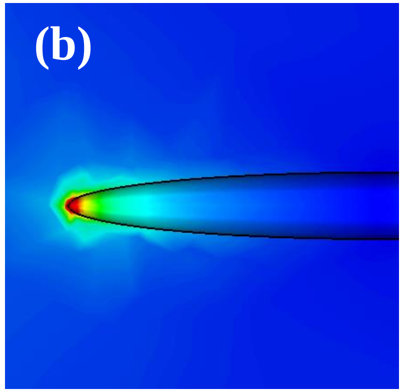

(c)

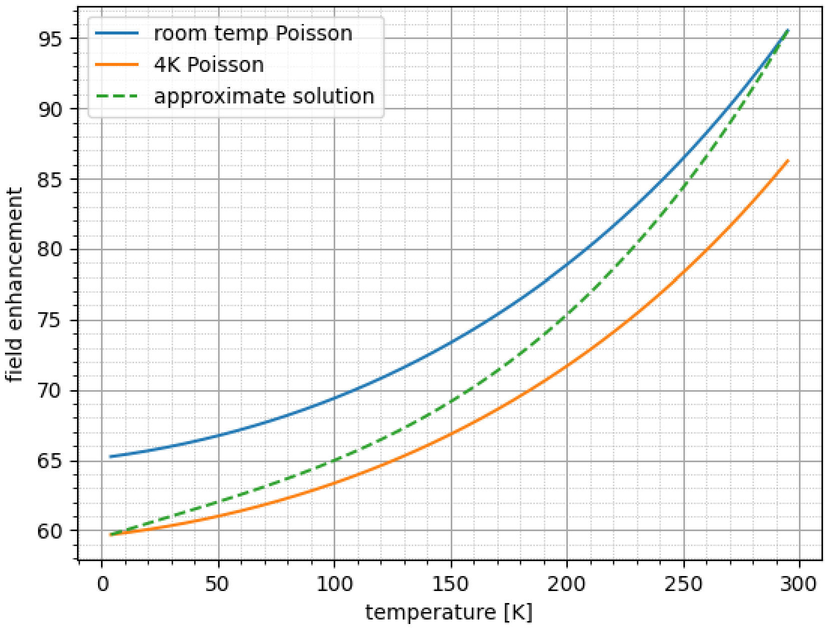

RF Heating

- Main gun section shown outside of cryostat (far left)
- Simplified thermal steady state simulation shown (middle) with previous cooling configuration to show accuracy of transient cooling simulations given estimated heat leaks from waveguide, beam pipe etc.
- RF heating over 6 hours (right) at 1 Hz ≈ 0.8 W

$$\Delta T(T) = \frac{R_s(T)\,|H_{||}|^2\sqrt{t}}{\sqrt{\pi\rho' c_\epsilon \sigma L T}} \propto \frac{R_s(T)}{\sqrt{\rho' c_\epsilon \sigma L T}} \propto \frac{R_s(T)}{\sqrt{\rho' c_\epsilon \sigma T}}$$

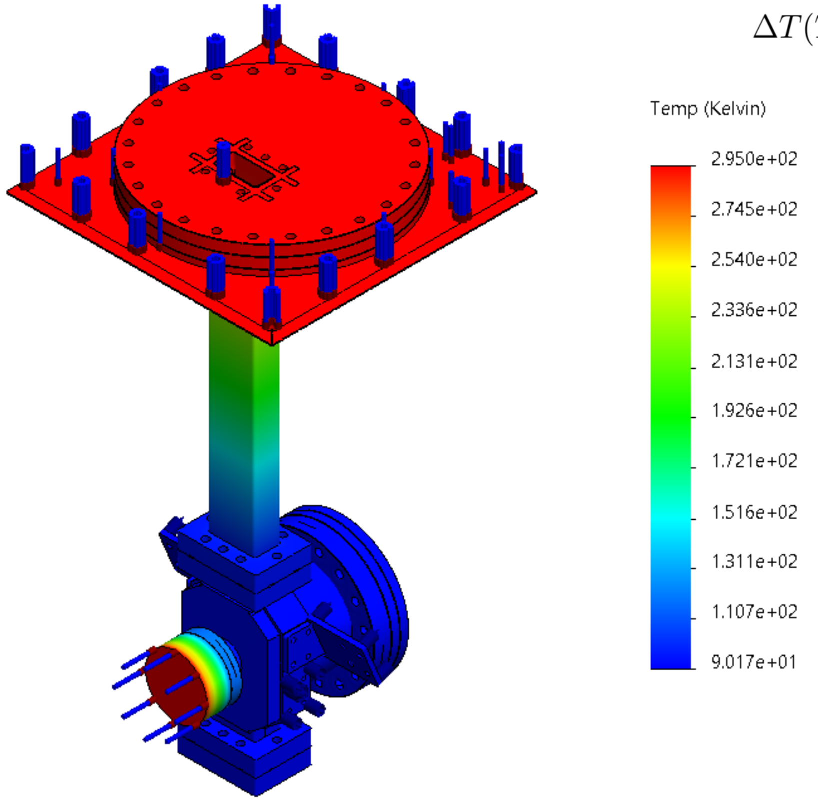

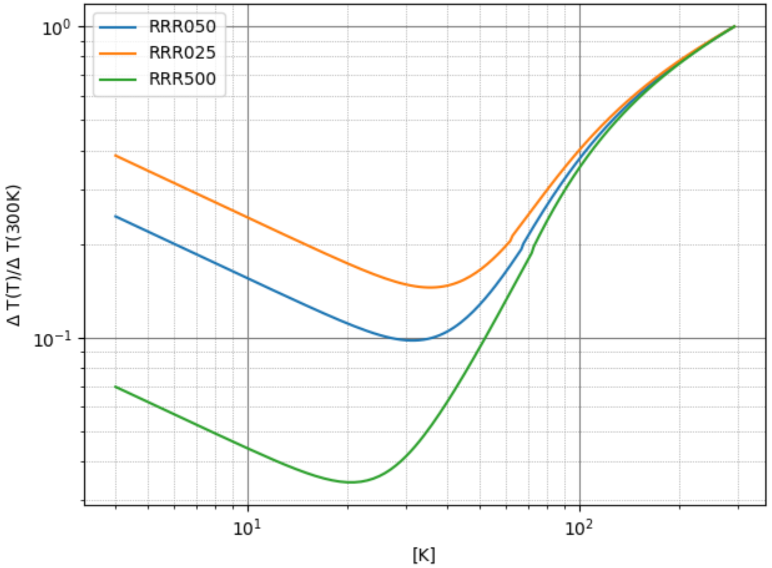

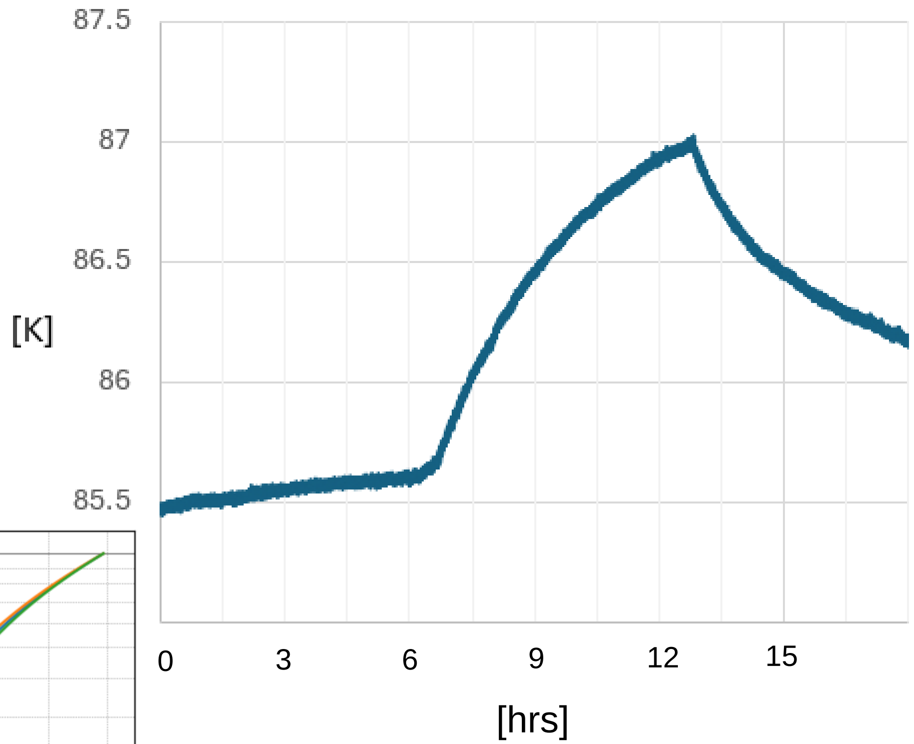

RF Heating

- Main gun section shown outside of cryostat (far left)
- Simplified thermal steady state simulation shown (middle) with previous cooling configuration to show accuracy of transient cooling simulations given estimated heat leaks from waveguide, beam pipe etc.
- RF heating over 6 hours (right) at 1 Hz ≈ 0.8 W

$$\Delta T(T) = \frac{R_s(T)\,|H_{||}|^2\sqrt{t}}{\sqrt{\pi\rho' c_\epsilon \sigma L T}} \propto \frac{R_s(T)}{\sqrt{\rho' c_\epsilon \sigma L T}} \propto \frac{R_s(T)}{\sqrt{\rho' c_\epsilon \sigma T}}$$

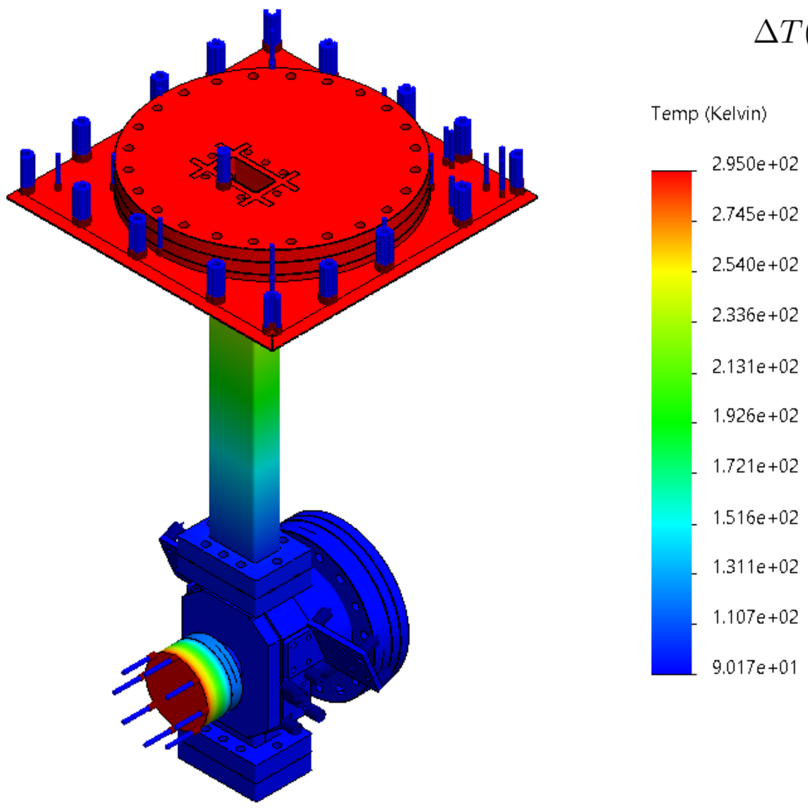

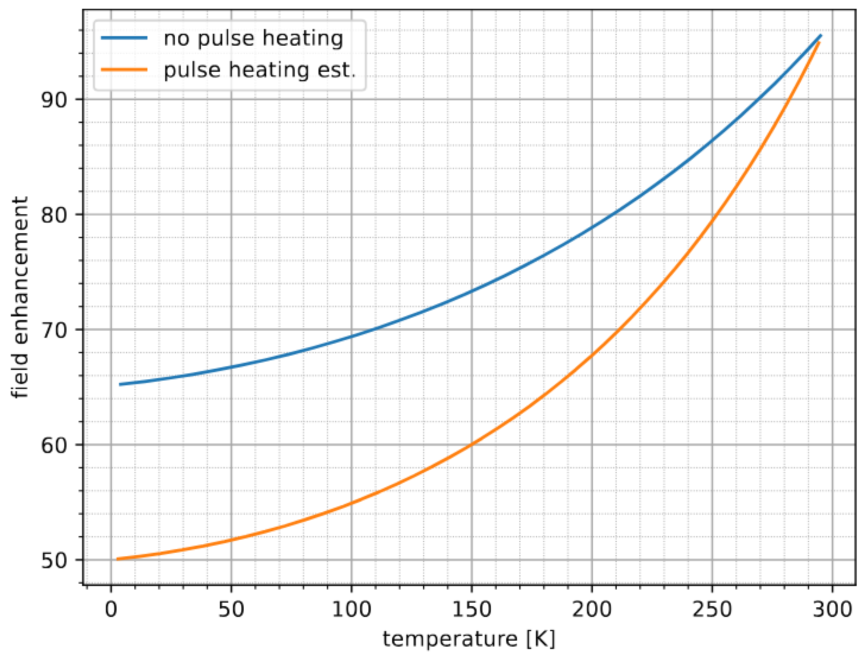

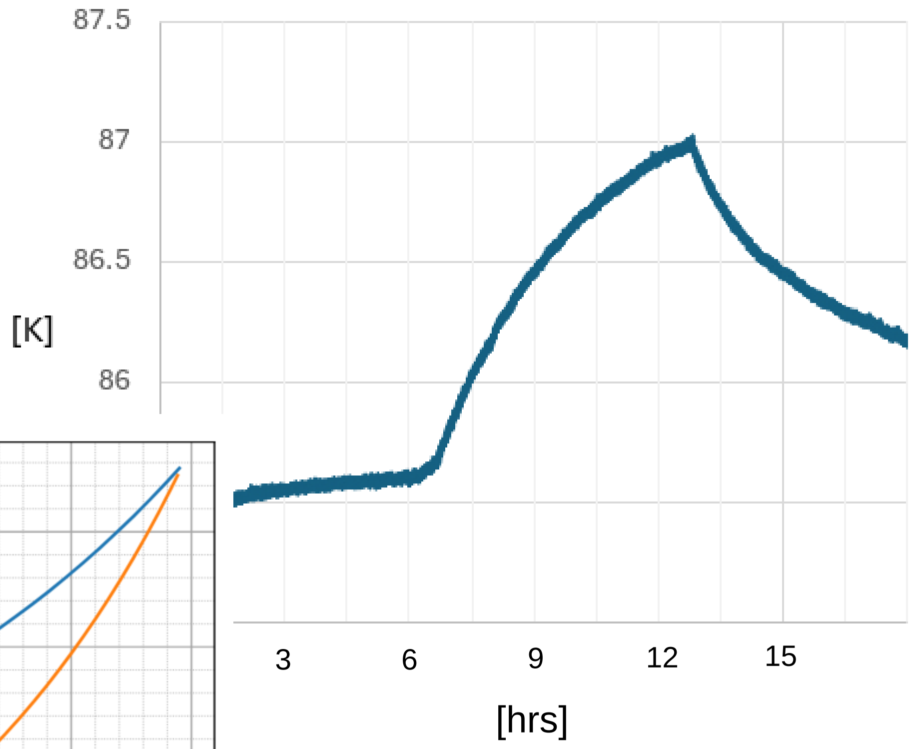

4. Cryo RF Performance Overview

- Parameters for gun thus far compared to RRR100-500 case (left) with empirical numbers measured to inform simulations (right)

Parameter	29
Frequency	5.(
Q_0	85
β	0.:
Filling time	-

E field magnitude

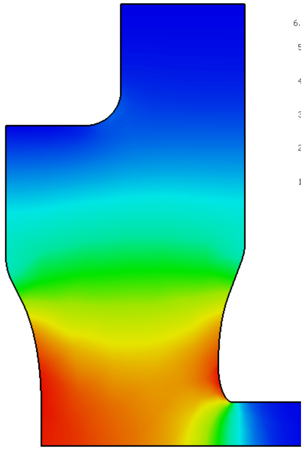

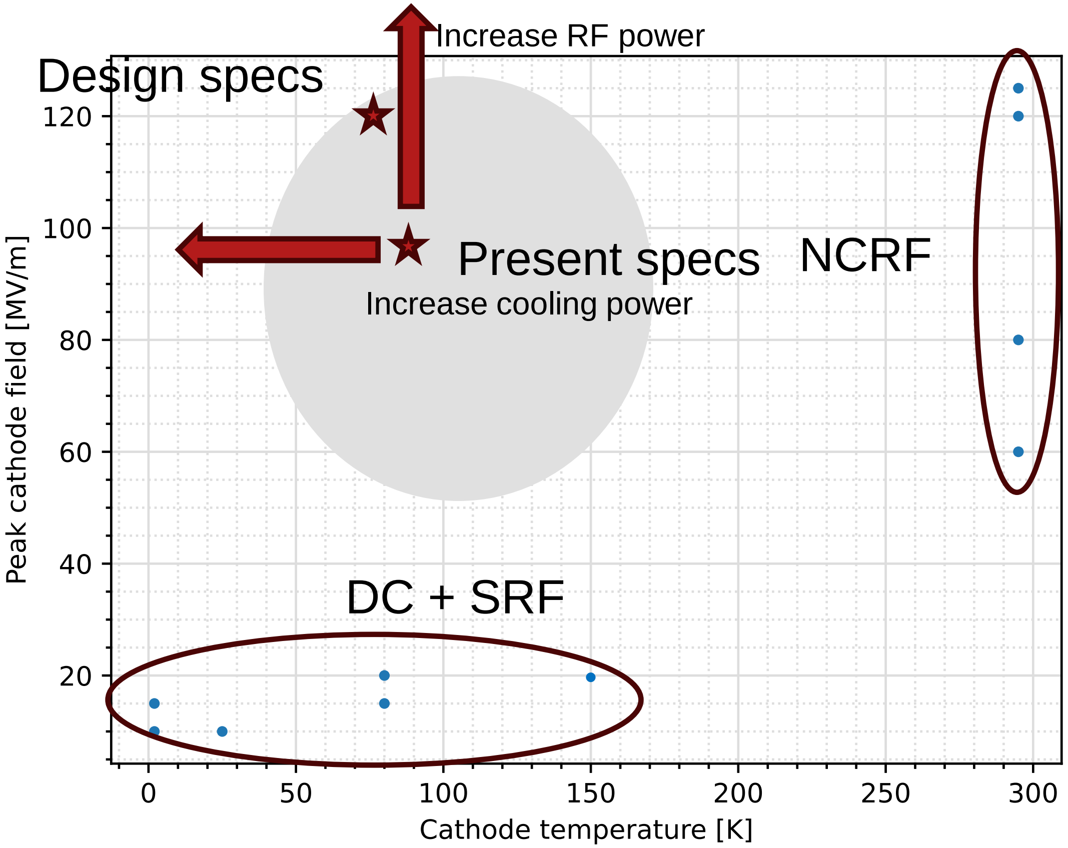

Lawler, G. E., et al. *Instruments* 8.1 (2024): 14.
Doi: 10.3390/instruments8010014

95 K	77K	45 K
5720.410 ± 0.003[1]	5721 ± 3	5722 ± 4
14326 ± 12[1]	21000 ± 3600	30000 ± 9900
1.069 ± 0.002[1]	1.60 ± 0.44	2.4 ± 0.9
0.386 ± 0.001[1]	0.44 ± 0.01	0.49 ± 0.03
0.85 ± 0.08	0.79 ± 0.01	0.70 ± 0.09
1.70 ± 0.02	1.58 ± 0.03	1.40 ± 0.19
92 ± 5 MV/m	93 ± 3 MV/m	102 ± 7 MV/m

measured or computed directly from low power measurements

CYBORG Function 2 (cont.)

- Future cathode integration creates additional need for understanding dark current
- INFN style shown in purple (right)
- Room temperature high gradient gun with RF knife edge in use at another UCLA beamline called PEGASUS (below)
  - Effective but limited to 80 MV/m of designed 120 MV/m for several reasons including additional dark current from cathode gap
- Scaled to CYBORG backplane (right) w/ field enhancements simulated along cathode plane

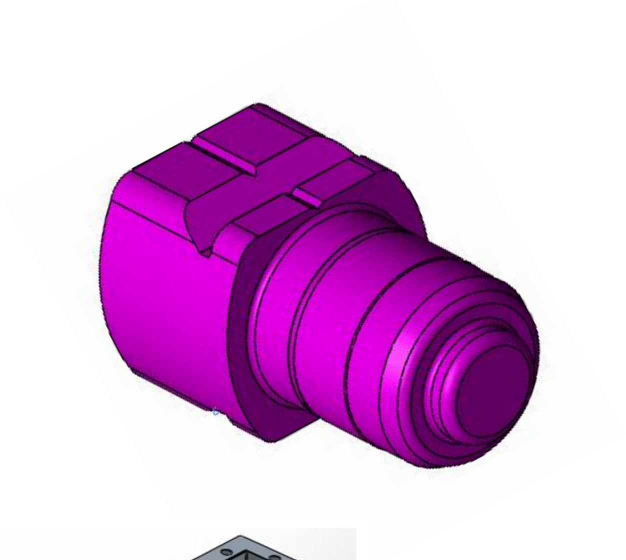

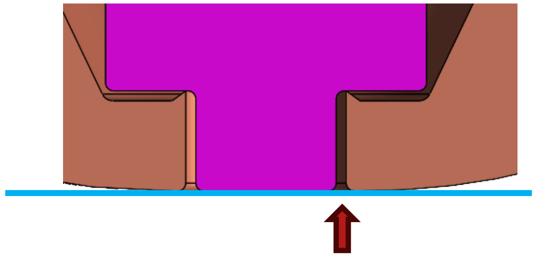

250 um gap at
room temp
245 um at 77 K

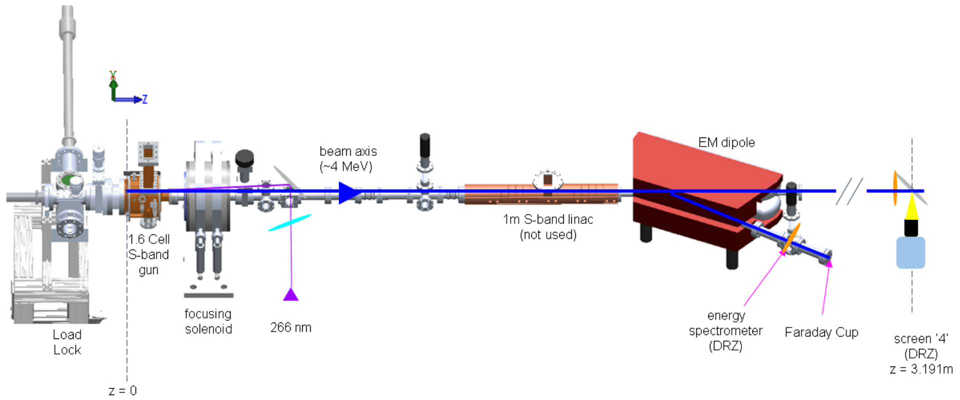

Alesini, David, et al. *Physical Review Special Topics-Accelerators and Beams* 18.9 (2015): 092001.
Doi: 10.1103/PhysRevSTAB.18.092001

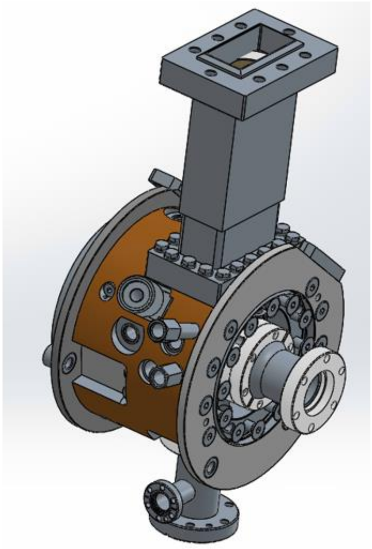

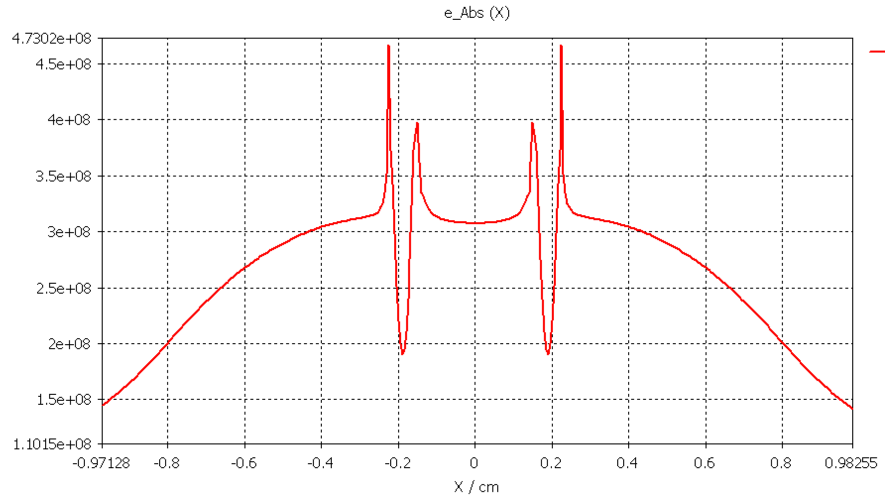

CYBORG UED

- C-band SLED RF amplifier for collaboration with SLAC => 2 MW output power
- Considering optimization with Cornell for UED with 180 MV/m peak cathode field
- Addition of X-band linearizer advantageous

- Low charge case for UED consideration
  - 75 um spot size; Cu cathode; 77 K; 0.015 mm mrad; 25 meV MTE;
  - Simulation @ 120 MV/m
    - 1 MeV
    - rms energy spread 3e-4
    - 0.063 mm mrad & 0.081 mm mrad
  - Simulation @ 240 MV/m
    - 2 MeV
    - rms energy spread 6e-4
    - 0.022 mm mrad & 0.025 mm mrad

TABLE II. The beam parameters at the sample in the velocity bunching scheme.

Beam Energy	3.5 MeV
rms relative energy spread	9×10^{-4}
bunch charge	50 fC (3×10^5 e^-)
normalized rms emittance	0.08 mm-mrad
transverse rms spot-size	0.25 mm
rms bunch length	4 fs

R. K. Li, P. Musumeci, H. A. Bender, N. S. Wilcox, M. Wu; *J. Appl. Phys.* 1 October 2011; 110 (7): 074512. https://doi.org/10.1063/1.3646465

Phase3

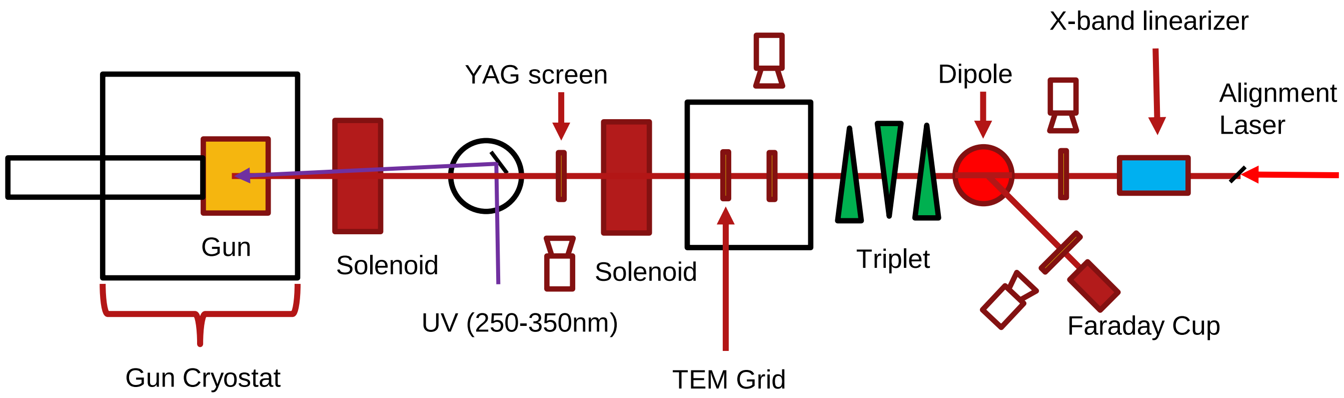

5. Conclusions

1. In BDR reduced high gradient environments dark current presence and impacts of dark current can be considered for high brightness applications
2. Shunt impedance optimized cavities seem to exasperate problem
3. Empirical cryogenic reduction could be advantageous for high gradient brightness operation complementary to BDR reduction alone
4. Capabilities to study increasing significantly at UCLA and LANL